TECHNISCHE UNIVERSITÄT
KAISERSLAUTERN

SCHRIFTEN ZUR

FUNKTIONALANALYSIS
UND GEOMATHEMATIK

P. Kammann, V. Michel

Time – Dependent Cauchy – Navier Splines and their Application to Seismic Wave Front Propagation

Bericht 26 – Juli 2006

FACHBEREICH MATHEMATIK

Time–Dependent Cauchy–Navier Splines and their Application to Seismic Wave Front Propagation

P. Kammann, V. Michel

Geomathematics Group
Department of Mathematics
University of Kaiserslautern
P.O. Box 3049
D–67653 Kaiserslautern, Germany
pkammann@mathematik.uni-kl.de, michel@mathematik.uni-kl.de

Abstract

In this paper a known orthonormal system of time– and space–dependent functions, that were derived out of the Cauchy–Navier equation for elastodynamic phenomena, is used to construct reproducing kernel Hilbert spaces. After choosing one of the spaces the corresponding kernel is used to define a function system that serves as a basis for a spline space. We show that under certain conditions there exists a unique interpolating or approximating, respectively, spline in this space with respect to given samples of an unknown function. The name "spline" here refers to its property of minimising a norm among all interpolating functions. Moreover, a convergence theorem and an error estimate relative to the point grid density are derived. As numerical example we investigate the propagation of seismic waves.

Key Words: reproducing kernel, spline, sphere, elasticity, seismic wave, Cauchy–Navier equation, time dependence.
AMS(2000) Classification: 65D07, 86A17, 41A05, 41A15, 41A52, 35L05.

1 Introduction

The use of reproducing kernels for generating interpolating or approximating structures has been investigated by a series of authors in the past (see, for example, [3, 8, 9, 10, 11, 12, 13, 19, 20]). Our interpolation and approximation method introduced here is motivated by the harmonic spline method introduced by W. Freeden (see [8, 9, 12, 14]) where certain Hilbert spaces $\mathcal{H}$ of functions on the unit sphere Ω in $\mathbb{R}^3$ are introduced that have a reproducing kernel $K_{\mathcal{H}}$. For interpolating or approximating a (harmonic) function $F : \Omega \to \mathbb{R}$ based on given values $\{F(\eta_k)\}_{k=1,\dots,N}$ a spline basis system $\{K_{\mathcal{H}}(\eta_k, \cdot)\}_{k=1,\dots,N}$ is constructed out of the reproducing kernel. Finally, a linear combination $S = \sum_{k=1}^{N} a_k K_{\mathcal{H}}(\eta_k, \cdot)$ is determined that satisfies the interpolation conditions or

minimises a certain functional in the approximation case. Due to smoothness and best approximation properties that can be proved for the solution S it is called (harmonic spherical) spline in a generalised abstract sense.
Some further developments of this approach have been realised in the meantime. In [11] the interpolation conditions $S(\eta_k) = F(\eta_k)$ are generalised to applications of functionals in the sense of $\mathcal{F}_k S = \mathcal{F}_k F$. This improvement then motivated the introduction of a corresponding spline method for harmonic functions on the ball in $\mathbb{R}^3$ instead of the sphere ([7, 24]). The discussed application is the recovery of the Earth's mass density distribution out of various satellite measurements of the gravitational field. Finally, in [13] the interpolation or approximation of functions on regular surfaces instead of spheres is treated.
We will show here that a similar spline method can be established for the Cauchy–Navier equation (in the isotropic, (layerwise) homogeneous case). For this purpose the time– and space–dependent function system derived in [16] is used to construct Sobolev–like Hilbert spaces that possess reproducing kernels. Based on this, spline basis functions are defined and existence and uniqueness results for the corresponding interpolation and approximation problem, respectively, are proved. Furthermore, minimum properties concerning the smoothness of the interpoland and its characterisation as best approximation can be shown. Moreover, a convergence theorem shows that by appropriately densifying the data grid the obtained sequence of splines (one spline per finite subgrid) converges to the function that has to be interpolated.
The introduced method contains several new features: First, it includes time–dependent modelling. Second, instead of the Laplace equation for harmonic functions it treats the more complicated Cauchy–Navier equation of elastodynamic phenomena. Note that a spline approach for the steady, i.e. time–independent, equation is derived in [22] and applied to the water load induced deformation of the ground surrounding an artificial lake. Third, the involved basis functions for the construction of the spaces are complex–valued. Due to those new constellations the transfer of the theorems and, in particular, their proofs to the modified situation turned out to be non–trivial. Nevertheless, corresponding results to the known spherical, time–independent, harmonic case can be derived.
In the numerical part of this paper we study waves that propagate through a 3–dimensional ball and that are sampled at its surface. First, we use two Gaussian bell functions, where one moves with the compressional wave speed and the other one with the shear wave speed. The advantage of this test is the fact that we globally know the wave function and are, thus, able to prove numerically the good approximation to the original function achieved by the spline. Due to those encouraging results we apply the method to realistic seismograms that are artificially generated by the software GEMINI (see [5]). In view of the intricate structure of seismic waves we obtain a very good visualisation of the propagating wave front.

2 Preliminaries

The letters $\mathbb{N}$, $\mathbb{N}_0$, $\mathbb{R}$, $\mathbb{R}^+$ and $\mathbb{C}$ denote the set of positive integers, non–negative integers, real numbers, positive real numbers and complex numbers, respectively, $\overline{z}$ represents the complex conjugate of $z \in \mathbb{C}$. The vector space $\mathbb{R}^3$ is equipped with the Euclidean scalar product $x \cdot y := x_1 y_1 + x_2 y_2 + x_3 y_3$, $x = (x_1, x_2, x_3)^{\mathrm{T}}$, $y = (y_1, y_2, y_3)^{\mathrm{T}} \in \mathbb{R}^3$, and the corresponding norm $|x| := \sqrt{x \cdot x}$. The vector product is defined by $x \wedge y = (x_2\, y_3 - x_3\, y_2\,, x_3\, y_1 - x_1\, y_3\,, x_1\, y_2 - x_2\, y_1)^{\mathrm{T}}$, $x, y \in \mathbb{R}^3$.
$\mathrm{C}^{(k)}(D, \mathbb{R}^n)$, $D \subset \mathbb{R}^m$, $k \in \mathbb{N}_0 \cup \{\infty\}$, $n, m \in \mathbb{N}$, denotes the set of all functions $f : D \to \mathbb{R}^n$ which are k–times continuously differentiable. The space $\mathrm{L}^2(D, \mathbb{C}^n)$, $D \subset \mathbb{R}^m$ (Lebesgue) measurable, $n, m \in \mathbb{N}$, of all equivalence classes of almost everywhere identical square–integrable functions

$f : D \to \mathbb{C}^n$ equipped with the scalar product

$$(f,g)_2 := (f,g)_{\mathrm{L}^2(D,\mathbb{C}^n)} := \int_D \sum_{i=1}^{n} F_i(x)\,\overline{G_i(x)}\,dx\,,$$

$$f,g \in \mathrm{L}^2(D,\mathbb{C}^n)\,,\ f=(F_1,\ldots,F_n)^{\mathrm{T}},\ g=(G_1,\ldots,G_n)^{\mathrm{T}},$$

is a Hilbert space. The corresponding norm is given by

$$\|f\|_2 := \|f\|_{\mathrm{L}^2(D,\mathbb{C}^n)} := \sqrt{(f,f)_{\mathrm{L}^2(D,\mathbb{C}^n)}}\ .$$

To simplify notations we will write $\mathrm{C}(D) := \mathrm{C}(D,\mathbb{R})$, $\mathrm{c}(D) := \mathrm{C}(D,\mathbb{R}^3)$, $\mathrm{L}^2(D) := \mathrm{L}^2(D,\mathbb{C})$, $\mathrm{l}^2(D) := \mathrm{L}^2(D,\mathbb{C}^3)$ etc. for $D \subset \mathbb{R}^m$. Analogously, we will denote scalar functions by capital letters and vectorial functions by lower–case letters.
We will restrict our attention to a spherical model of the Earth denoted by $\overline{\Omega_r^{\mathrm{int}}}$ which is the closed inner space of the sphere with radius $r \in \mathbb{R}^+$, $\Omega_r = \{x \in \mathbb{R}^3 : |x| = r\}$. $\Omega := \Omega_1$ denotes the unit sphere.
As usual, the gradient operator is denoted by ∇ or grad and the Laplace operator by Δ. The gradient can be decomposed into a radial part and an angular part:

$$\nabla_{r\xi} = \xi\frac{\partial}{\partial r} + \frac{1}{r}\nabla^*_\xi\,, \quad r \in \mathbb{R}^+\,, \xi \in \Omega\,.$$

where ∇^* is the surface gradient on the unit sphere Ω. The surface curl gradient L^* is defined by

$$L^*_\xi F(\xi) := \xi \wedge \nabla^*_\xi F(\xi)\,, \quad \xi \in \Omega\,,\ F \in \mathrm{C}^{(1)}(\Omega).$$

The divergence of a vector field $f \in \mathrm{c}^{(1)}(D)$, $D \subset \mathbb{R}^3$, is defined by

$$\operatorname{div} f := \nabla \cdot f := \sum_{j=1}^{3} \frac{\partial F_j}{\partial x_j}\,, \quad f = (F_1,F_2,F_3)^{\mathrm{T}}.$$

An important role in the theory of functions on the sphere plays the space $\mathrm{Harm}_n(\Omega)$ of spherical harmonics, i.e. homogeneous harmonic polynomials of degree $n \in \mathbb{N}_0$ restricted to the unit sphere Ω. This space has the dimension $2n+1$ such that we are able to assume that a complete $\mathrm{L}^2(\Omega)$–orthonormal system $\{Y_{n,j}\}_{j=1,\ldots,2n+1}$ in $\mathrm{Harm}_n(\Omega)$ is given. Since two spherical harmonics $Y_n \in \mathrm{Harm}_n(\Omega)$, $Y_m \in \mathrm{Harm}_m(\Omega)$ of different degrees $n \neq m$ are always orthogonal the whole system $\{Y_{n,j}\}_{n\in\mathbb{N}_0,j=1,\ldots,2n+1}$ is automatically an orthonormal system in $\mathrm{L}^2(\Omega)$. Moreover, one can prove that such a system is also complete.
Using the scalar system $\{Y_{n,j}\}_{n\in\mathbb{N}_0,j=1,\ldots,2n+1}$ we obtain a complete orthonormal vectorial system $\{y^{(i)}_{n,j}\}_{i=1,2,3,n\geq 0_i,j=1,\ldots,2n+1}$ in $\mathrm{l}^2(\Omega)$, given by

$$y^{(i)}_{n,j} := \left(\mu^{(i)}_n\right)^{-1/2} o^{(i)} Y_{n,j}\ , \quad j=1,\ldots,2n+1\,,\ n \geq 0_i := \begin{cases} 0 & \text{if } i=1 \\ 1 & \text{if } i=2,3 \end{cases}\ ,$$

where the operators $o^{(i)}$, $i=1,2,3$, are defined by

$$\begin{aligned} o^{(1)}_\xi F(\xi) &= \xi F(\xi)\,, \\ o^{(2)}_\xi F(\xi) &= \nabla^*_\xi F(\xi)\,, \\ o^{(3)}_\xi F(\xi) &= L^*_\xi F(\xi)\,, \quad \xi \in \Omega\,,\ F \in \mathrm{C}^{(1)}(\Omega), \end{aligned}$$

and the normalising constants $\left(\mu_n^{(i)}\right)^{-1/2}$, $i = 1, 2, 3,\ n \geq 0_i$, are given by

$$\mu_n^{(i)} := \left\| o^{(i)} Y_{n,j} \right\|^2_{l^2(\Omega)} = \begin{cases} 1 & \text{if } i = 1 \\ n(n+1) & \text{if } i = 2, 3 \end{cases} .$$

There exists one and only one system of polynomials $\{P_n\}_{n\in\mathbb{N}_0}$ which satisfies the following properties for all $n \in \mathbb{N}_0$:

(i) P_n is a polynomial of degree n, defined on $[-1, 1]$,

(ii) $\int_{-1}^{1} P_n(t)P_m(t)\,dt = 0 \quad \textit{for all } m \in \mathbb{N}_0\backslash\{n\}$,

(iii) $P_n(1) = 1$.

These polynomials P_n, $n \in \mathbb{N}_0$, are called Legendre polynomials. Their $\mathrm{L}^2([-1, 1])$–norm is given by

$$\|P_n\|_{\mathrm{L}^2([-1,1])} = \left(\int_{-1}^{1} (P_n(t))^2 dt \right)^{1/2} = \sqrt{\frac{2}{2n+1}} \ , \ n \in \mathbb{N}_0 \ .$$

3 A Function System for the Cauchy–Navier Equation

The Cauchy–Navier equation for an isotropic, homogeneous ball without body forces is given by

$$\varrho \, \frac{\partial^2 u}{\partial t^2} = (\lambda + \mu) \, \mathrm{grad}_x \, \mathrm{div}_x \, u + \mu \Delta_x u \ , \tag{1}$$

where ϱ is the scalar density and $\lambda, \mu > 0$ are the so–called Lamé parameters, which are here constant since we consider the homogeneous case. The unknown quantity $u : \mathbb{R} \times \overline{\Omega_r^{\mathrm{int}}} \to \mathbb{R}^3$ is a small displacement depending on time $t \in \mathbb{R}$ and position $x \in \overline{\Omega_r^{\mathrm{int}}}$, $r \in \mathbb{R}^+$.

A fundamental system for the Fourier–transformed, i.e. frequency–dependent, form is given by the so–called Hansen vectors (see e.g. [2]). We use here inverse Fourier transforms of those functions derived in [16]:

$$\begin{aligned}
\hat{\mathfrak{l}}_{n,j}(t, r\xi) &= \Bigg(-\frac{1}{2} \left(\frac{\alpha}{r}\right)^2 (-i)^{n+1} \, t P_n \left(-\frac{\alpha}{r} t\right) y_{n,j}^{(1)}(\xi) \\
&\quad + (-1)^n \frac{\alpha}{2r} i^{\,n-1} P_n \left(-\frac{\alpha}{r} t\right) \sqrt{n(n+1)}\, y_{n,j}^{(2)}(\xi) \Bigg) \chi_{\left]-\frac{r}{\alpha}, \frac{r}{\alpha}\right[}(t) \ , \\
&\quad |t| \neq \frac{r}{\alpha} \, , \ \xi \in \Omega \, , \ n \in \mathbb{N}_0 \, , \ j \in \{1, \ldots, 2n+1\} \ , \\
\hat{\mathfrak{m}}_{n,j}(t, r\xi) &= \frac{\beta}{2r} (-i)^n \, P_n \left(-\frac{\beta}{r} t\right) y_{n,j}^{(3)}(\xi) \, \chi_{\left]-\frac{r}{\beta}, \frac{r}{\beta}\right[}(t) \ , \\
&\quad |t| \neq \frac{r}{\beta} \, , \ \xi \in \Omega \, , \ n \in \mathbb{N} \, , \ j \in \{1, \ldots, 2n+1\} \ , \\
\hat{\mathfrak{n}}_{n,j}(t, r\xi) &= \Bigg(\frac{(-i)^{n-1}\beta}{(2n+1)2r} \left((n+1) P_{n-1} \left(-\frac{\beta}{r} t\right) + n P_{n+1} \left(-\frac{\beta}{r} t\right) \right) \sqrt{n(n+1)}\, y_{n,j}^{(2)}(\xi) \\
&\quad + \frac{1}{2} (-1)^n \, n(n+1) \, \frac{\beta}{r} i^{\,n-1} P_n \left(-\frac{\beta}{r} t\right) y_{n,j}^{(1)}(\xi) \Bigg) \chi_{\left]-\frac{r}{\beta}, \frac{r}{\beta}\right[}(t) \ , \\
&\quad |t| \neq \frac{r}{\beta} \, , \ \xi \in \Omega \, , \ n \in \mathbb{N} \, , \ j \in \{1, \ldots, 2n+1\} \ ,
\end{aligned}$$

where $\chi_D : \mathbb{R} \to \mathbb{R}$ is the characteristic function, defined by

$$\chi_D(t) := \begin{cases} 1\,, & t \in D \\ 0\,, & t \notin D \end{cases}$$

and i is the imaginary unit. The constants $\alpha > \beta > 0$ denote the velocities of compressional and shear body waves, respectively, given by $\alpha = \sqrt{(\lambda + 2\mu)/\varrho}$ and $\beta = \sqrt{\mu/\varrho}$.
From [16] we know that the obtained functions are orthogonal in $\mathrm{l}^2(\mathbb{R} \times \overline{\Omega_r^{\mathrm{int}}})$. In the following we will consider only the normal parts of the functions and restrict them to $\left]-\frac{r}{\beta}, \frac{r}{\beta}\right[\times \Omega_r$. Therefore, the solutions are projected on $\xi \in \Omega$ and we obtain the functions $L_{n,j}$, $M_{n,j}$, and $N_{n,j}$ which are elements of $\mathrm{L}^2\big(\left]-\frac{r}{\beta}, \frac{r}{\beta}\right[\times \Omega_r\big)$:

$$\begin{aligned}
L_{n,j}(t, r\xi) &:= \xi \cdot \hat{\mathfrak{l}}_{n,j}(t, r\xi) \\
&= -\frac{1}{2}\left(\frac{\alpha}{r}\right)^2 (-i)^{n+1}\, t\, P_n\left(-\frac{\alpha}{r}t\right) Y_{n,j}(\xi)\, \chi_{\left]-\frac{r}{\alpha}, \frac{r}{\alpha}\right[}(t)\,, \\
M_{n,j}(t, r\xi) &:= \xi \cdot \hat{\mathfrak{m}}_{n,j}(t, r\xi) = 0\,, \\
N_{n,j}(t, r\xi) &:= \xi \cdot \hat{\mathfrak{n}}_{n,j}(t, r\xi) \\
&= (-1)^n\, \frac{1}{2}\, n(n+1) \frac{\beta}{r}\, i^{n-1} P_n\left(-\frac{\beta}{r}t\right) Y_{n,j}(\xi)\,,
\end{aligned}$$

$j \in \{1, \ldots, 2n+1\}$, where $n \in \mathbb{N}_0$ in case of $L_{n,j}$ and $n \in \mathbb{N}$ in case of $M_{n,j}$ and $N_{n,j}$. Note that the functions $\hat{\mathfrak{m}}_{n,j}$ do not have normal parts.
To prove that the remaining functions are still orthogonal in $\mathrm{L}^2\big(\left]-\frac{r}{\beta}, \frac{r}{\beta}\right[\times \Omega_r\big)$, we have the following theorem.

Theorem 1 *The function system* $\{L_{n,j}\}_{n\in\mathbb{N}_0, j=1,\ldots,2n+1} \cup \{N_{n,j}\}_{n\in\mathbb{N}, j=1,\ldots,2n+1}$ *is orthogonal with respect to* $\mathrm{L}^2\big(\left]-\frac{r}{\beta}, \frac{r}{\beta}\right[\times \Omega_r\big)$.

Proof. Obviously,

$$\begin{aligned}
(L_{n,j}, L_{m,k})_{\mathrm{L}^2\left(\left]-\frac{r}{\beta}, \frac{r}{\beta}\right[\times \Omega_r\right)} &= (N_{n,j}, N_{m,k})_{\mathrm{L}^2\left(\left]-\frac{r}{\beta}, \frac{r}{\beta}\right[\times \Omega_r\right)} \\
&= (L_{n,j}, N_{m,k})_{\mathrm{L}^2\left(\left]-\frac{r}{\beta}, \frac{r}{\beta}\right[\times \Omega_r\right)} = 0
\end{aligned}$$

for $n \neq m$ or $j \neq k$, due to the $\mathrm{L}^2(\Omega_r)$–orthogonality of $\{Y_{n,j}\}_{n\in\mathbb{N}_0, j=1,\ldots,2n+1}$. It remains to show that

$$(L_{n,j}, N_{n,j})_{\mathrm{L}^2\left(\left]-\frac{r}{\beta}, \frac{r}{\beta}\right[\times \Omega_r\right)} = 0\,,$$

which is fulfilled since

$$\int_{-r/\alpha}^{r/\alpha} t\, P_n\left(-\frac{\alpha}{r}t\right) P_n\left(-\frac{\beta}{r}t\right) dt = 0$$

(see [16], p. 538). ∎

To provide orthonormality we need the norms of the ansatz functions.

Theorem 2 *The* $\mathrm{L}^2\big(\left]-\frac{r}{\beta}, \frac{r}{\beta}\right[\times \Omega_r\big)$*–norms of* $L_{n,j}$ *and* $N_{n,j}$ *have the following properties:*

$$\begin{aligned}
\|L_{n,j}\|^2_{\mathrm{L}^2\left(\left]-\frac{r}{\beta}, \frac{r}{\beta}\right[\times \Omega_r\right)} &= \frac{r\alpha}{4}\left(\left(\frac{n+1}{2n+1}\right)^2 \frac{2}{2n+3} + \left(\frac{n}{2n+1}\right)^2 \frac{2}{2n-1}\right)\,, \\
&\quad n \in \mathbb{N}_0\,,\ j \in \{1, \ldots, 2n+1\}\,, \\
\|N_{n,j}\|^2_{\mathrm{L}^2\left(\left]-\frac{r}{\beta}, \frac{r}{\beta}\right[\times \Omega_r\right)} &= \frac{r\beta\, n^2(n+1)^2}{2(2n+1)}\,,\ n \in \mathbb{N}\,,\ j \in \{1, \ldots, 2n+1\}\,.
\end{aligned}$$

Proof. We have

$$\begin{aligned}\|L_{n,j}\|^2_{\mathrm{L}^2(]-\frac{r}{\beta},\frac{r}{\beta}[\times\Omega_r)} &= \int_{-r/\beta}^{r/\beta}\int_{\Omega_r}|L_{n,j}(t,x)|^2 d\omega_r(x)\,dt\\ &= \frac{\alpha^4}{4\,r^4}\int_{-r/\alpha}^{r/\alpha}\left(tP_n\left(-\frac{\alpha}{r}t\right)\right)^2\int_{\Omega_r}\left(Y_{n,j}\left(\frac{x}{|x|}\right)\right)^2 d\omega_r(x)\,dt\\ &= r^2\frac{\alpha^4}{4\,r^4}\int_{-r/\alpha}^{r/\alpha}\left(tP_n\left(-\frac{\alpha}{r}t\right)\right)^2 dt\ .\end{aligned}$$

From [16], p. 537, we obtain

$$\int_{-r/\alpha}^{r/\alpha}\left(tP_n\left(-\frac{\alpha}{r}t\right)\right)^2 dt = \frac{r^3}{\alpha^3}\left(\left(\frac{n+1}{2n+1}\right)^2\frac{2}{2n+3}+\left(\frac{n}{2n+1}\right)^2\frac{2}{2n-1}\right)\ .$$

Thus, we receive

$$\|L_{n,j}\|^2_{\mathrm{L}^2(]-\frac{r}{\beta},\frac{r}{\beta}[\times\Omega_r)} = \frac{r\alpha}{4}\left(\left(\frac{n+1}{2n+1}\right)^2\frac{2}{2n+3}+\left(\frac{n}{2n+1}\right)^2\frac{2}{2n-1}\right)\ .$$

Similarly, we obtain for $N_{n,j}$

$$\begin{aligned}\|N_{n,j}\|^2_{\mathrm{L}^2(]-\frac{r}{\beta},\frac{r}{\beta}[\times\Omega_r)} &= \int_{-r/\beta}^{r/\beta}\int_{\Omega_r}|N_{n,j}(t,x)|^2 d\omega_r(x)\,dt\\ &= \frac{\beta^2}{4\,r^2}\,n^2(n+1)^2\int_{-r/\beta}^{r/\beta}\left(P_n\left(-\frac{\beta}{r}t\right)\right)^2\int_{\Omega_r}\left(Y_{n,j}\left(\frac{x}{|x|}\right)\right)^2 d\omega_r(x)\,dt\\ &= r^2\frac{\beta^2}{4\,r^2}\,n^2(n+1)^2\int_{-r/\beta}^{r/\beta}\left(P_n\left(-\frac{\beta}{r}t\right)\right)^2 dt\\ &= \frac{r\beta}{4}\,n^2(n+1)^2\int_{-1}^{1}(P_n(\tau))^2 d\tau\\ &= \frac{r\beta\,n^2(n+1)^2}{2(2n+1)}\ .\end{aligned}$$

■

Finally, we normalise the orthogonal system under consideration.

Definition 3 *We define the following functions in* $\mathrm{L}^2(\,]-\frac{r}{\beta},\frac{r}{\beta}[\,\times\Omega_r)$*:*

$$\begin{aligned}U^{(1)}_{n,j} &:= \|L_{n,j}\|^{-1}_{\mathrm{L}^2(]-\frac{r}{\beta},\frac{r}{\beta}[\times\Omega_r)}L_{n,j}\ ,\quad n\in\mathbb{N}_0\,,\ j\in\{1,\dots,2n+1\}\ ,\\ U^{(2)}_{n,j} &:= \|N_{n,j}\|^{-1}_{\mathrm{L}^2(]-\frac{r}{\beta},\frac{r}{\beta}[\times\Omega_r)}N_{n,j}\ ,\quad n\in\mathbb{N}\,,\ j\in\{1,\dots,2n+1\}\ .\end{aligned}$$

We additionally define

$$U^{(2)}_{0,1}(t,r\xi) := \left(\frac{\beta}{2r^3}\right)^{1/2}\frac{1}{i\sqrt{4\pi}}\ .$$

The space CN *is defined by*

$$\mathrm{CN} := \overline{\mathrm{span}\left\{U^{(i)}_{n,j}\right\}_{i=1,2,n\in\mathbb{N}_0,j=1,\dots 2n+1}}^{\|\cdot\|_{\mathrm{L}^2(]-\frac{r}{\beta},\frac{r}{\beta}[\times\Omega_r)}}\ .$$

Note that the functions $U^{(1)}_{n,j}(t,x)$, $n\in\mathbb{N}_0$, $j=1,\dots 2n+1$, are discontinuous for $t\in\left\{-\frac{r}{\alpha},\frac{r}{\alpha}\right\}$.

4 Sobolev Spaces

We will now introduce so–called Sobolev spaces which are certain Hilbert spaces possessing a reproducing kernel. The following derivation is motivated by an approach for the Laplace equation in [8, 9, 12, 14]. We start our considerations with the linear space $\mathcal{A}$ consisting of all sequences $\{A_n\}_{n\in\mathbb{N}_0}$ of real numbers $A_n,\ n \in \mathbb{N}_0$:

$$\mathcal{A} = \{\{A_n\}_{n\in\mathbb{N}_0} \mid \ A_n \in \mathbb{R}\} \ .$$

Let $\{A_n\} := \{A_n\}_{n\in\mathbb{N}_0}$ be a sequence in $\mathcal{A}$. We split $\mathbb{N}_0$ into two parts such that $\mathbb{N}_0 = \mathcal{N} \cup \mathcal{N}_0$, $\mathcal{N} \cap \mathcal{N}_0 = \emptyset$, where

$$\begin{aligned} \mathcal{N} &= \{n \in \mathbb{N}_0 \mid A_n \neq 0\} \ , \\ \mathcal{N}_0 &= \{n \in \mathbb{N}_0 \mid A_n = 0\} \ . \end{aligned}$$

Consider the set $\mathcal{E} = \mathcal{E}\big(\{A_n\}; \left]-\frac{r}{\beta}, \frac{r}{\beta}\right[\times \Omega_r\big)$ of all functions $F \in \mathrm{CN}$, i.e. $F : \left]-\frac{r}{\beta}, \frac{r}{\beta}\right[\times \Omega_r \to \mathbb{C}$ of the form

$$F = \sum_{n=0}^{\infty} \sum_{j=1}^{2n+1} \left(F^{\wedge}(n,j,1)\, U_{n,j}^{(1)} + F^{\wedge}(n,j,2)\, U_{n,j}^{(2)} \right) \tag{2}$$

with

$$F^{\wedge}(n,j,i) = \left(F, U_{n,j}^{(i)} \right)_{\mathrm{L}^2\left(\left]-\frac{r}{\beta}, \frac{r}{\beta}\right[\times \Omega_r\right)} \ ,$$

satisfying

$$F^{\wedge}(n,j,i) = 0 \quad \text{for all } n \in \mathcal{N}_0$$

and

$$\sum_{n\in\mathcal{N}} \sum_{j=1}^{2n+1} \sum_{i=1}^{2} A_n^2 \left| F^{\wedge}(n,j,i) \right|^2 < +\infty \ .$$

We can define an inner product $(\cdot,\cdot)_{\mathcal{H}\left(\{A_n\}; \left]-\frac{r}{\beta}, \frac{r}{\beta}\right[\times \Omega_r\right)}$ on $\mathcal{E}$ by

$$(F,G)_{\mathcal{H}\left(\{A_n\}; \left]-\frac{r}{\beta}, \frac{r}{\beta}\right[\times \Omega_r\right)} := \sum_{n\in\mathcal{N}} \sum_{j=1}^{2n+1} \sum_{i=1}^{2} A_n^2 F^{\wedge}(n,j,i)\, \overline{G^{\wedge}(n,j,i)} \ ,$$

where the Cauchy–Schwarz inequality gives us the finiteness of the right hand series (see e.g. [12]). The associated norm is given by

$$\|F\|_{\mathcal{H}\left(\{A_n\}; \left]-\frac{r}{\beta}, \frac{r}{\beta}\right[\times \Omega_r\right)} = \left((F,F)_{\mathcal{H}\left(\{A_n\}; \left]-\frac{r}{\beta}, \frac{r}{\beta}\right[\times \Omega_r\right)} \right)^{1/2} \ .$$

Definition 4 *Let $\{A_n\} \in \mathcal{A}$. The Sobolev space $\mathcal{H}\big(\{A_n\}; \left]-\frac{r}{\beta}, \frac{r}{\beta}\right[\times \Omega_r\big)$ is defined as the completion of $\mathcal{E}\big(\{A_n\}; \left]-\frac{r}{\beta}, \frac{r}{\beta}\right[\times \Omega_r\big)$ with respect to $(\cdot,\cdot)_{\mathcal{H}\left(\{A_n\}; \left]-\frac{r}{\beta}, \frac{r}{\beta}\right[\times \Omega_r\right)}$.*

$\mathcal{H}\big(\{A_n\}; \left]-\frac{r}{\beta}, \frac{r}{\beta}\right[\times \Omega_r\big)$ equipped with the inner product $(\cdot,\cdot)_{\mathcal{H}\left(\{A_n\}; \left]-\frac{r}{\beta}, \frac{r}{\beta}\right[\times \Omega_r\right)}$ is a Hilbert space. Further on we write $\mathcal{H}$ instead of $\mathcal{H}\big(\{A_n\}; \left]-\frac{r}{\beta}, \frac{r}{\beta}\right[\times \Omega_r\big)$ if no confusion is likely to arise.

A lemma related to a fundamental result due to Sobolev (see e.g. [23]) says that under certain circumstances the series expansion (2) converges uniformly to a function in ordinary sense.

Definition 5 *A sequence $\{A_n\} \in \mathcal{A}$ is said to be summable if*

$$\sum(\{A_n\}) := \sum_{n\in\mathcal{N}} \frac{2n+1}{4\pi} A_n^{-2} r^{-2} \times \left[\left(\left(\frac{n+1}{2n+1}\right)^2 \frac{2}{2n+3} + \left(\frac{n}{2n+1}\right)^2 \frac{2}{2n-1} \right)^{-1} \frac{\alpha}{r} + \frac{1}{2}(2n+1)\frac{\beta}{r} \right] < +\infty \, .$$

Note that $\{A_n\}$ is summable if and only if

$$\sum_{n\in\mathcal{N}} n^2 A_n^{-2} < +\infty \, .$$

Lemma 6 (Sobolev Lemma) *Let $\{A_n\} \in \mathcal{A}$ be summable. Then each $F \in \mathcal{H}$ corresponds to a function on $\left]-\frac{r}{\beta},\frac{r}{\beta}\right[\times \Omega_r$, which is continuous on $\left(\left]-\frac{r}{\beta},\frac{r}{\beta}\right[\setminus \left\{-\frac{r}{\alpha},\frac{r}{\alpha}\right\}\right) \times \Omega_r$.*

Proof. Let $t \in \left]-\frac{r}{\beta},\frac{r}{\beta}\right[$ and $x = r\xi \in \Omega_r$. Application of the Cauchy–Schwarz inequality yields for $F \in \mathcal{H}$, $N \in \mathbb{N}$ the estimate

$$\begin{aligned}
\left| \sum_{\substack{n\in\mathcal{N}\\ n\geq N}} \sum_{j=1}^{2n+1} \sum_{i=1}^{2} F^{\wedge}(n,j,i)\, U_{n,j}^{(i)}(t,x) \right|^2 &= \left| \sum_{\substack{n\in\mathcal{N}\\ n\geq N}} \sum_{j=1}^{2n+1} \sum_{i=1}^{2} A_n^{-1} U_{n,j}^{(i)}(t,x)\, A_n\, F^{\wedge}(n,j,i) \right|^2 \\
&\leq \left(\sum_{\substack{n\in\mathcal{N}\\ n\geq N}} \sum_{j=1}^{2n+1} \sum_{i=1}^{2} A_n^{-2} \left| U_{n,j}^{(i)}(t,x) \right|^2 \right) \left(\sum_{\substack{n\in\mathcal{N}\\ n\geq N}} \sum_{j=1}^{2n+1} \sum_{i=1}^{2} A_n^2 \left| F^{\wedge}(n,j,i) \right|^2 \right) \\
&\leq \left(\sum_{\substack{n\in\mathcal{N}\\ n\geq N}} A_n^{-2} \frac{2n+1}{4\pi} P_n(\xi^2) \frac{1}{r^2} \left[\left(\left(\frac{n+1}{2n+1}\right)^2 \frac{2}{2n+3} + \left(\frac{n}{2n+1}\right)^2 \frac{2}{2n-1} \right)^{-1} \right. \right. \\
&\quad \left. \left. \times \left(\frac{\alpha}{r}\right)^3 t^2 P_n^2\left(-\frac{\alpha}{r}t\right) \chi^2{}_{\left]-\frac{r}{\alpha},\frac{r}{\alpha}\right[}(t) + \frac{1}{2}(2n+1)\frac{\beta}{r} P_n^2\left(-\frac{\beta}{r}t\right) \right] \right) \|F\|_{\mathcal{H}}^2 \\
&\leq \left(\sum_{\substack{n\in\mathcal{N}\\ n\geq N}} A_n^{-2} \frac{2n+1}{4\pi} \frac{1}{r^2} \left[\left(\left(\frac{n+1}{2n+1}\right)^2 \frac{2}{2n+3} + \left(\frac{n}{2n+1}\right)^2 \frac{2}{2n-1} \right)^{-1} \frac{\alpha}{r} \right. \right. \\
&\quad \left. \left. + \frac{1}{2}(2n+1)\frac{\beta}{r} \right] \right) \|F\|_{\mathcal{H}}^2 \to 0 \text{ for } N \to \infty \, ,
\end{aligned}$$

where the series converges uniformly with respect to $(t,x) \in \left]-\frac{r}{\beta},\frac{r}{\beta}\right[\times \Omega_r$ due to the summability condition. Therefore, F is necessarily continuous where the functions $U_{n,j}^{(i)}$ are continuous, i.e. on $\left(\left]-\frac{r}{\beta},\frac{r}{\beta}\right[\setminus \left\{-\frac{r}{\alpha},\frac{r}{\alpha}\right\}\right) \times \Omega_r$. ∎

Furthermore, with summable sequences we can introduce reproducing kernels for Sobolev spaces.

Theorem 7 *Let $\{A_n\} \in \mathcal{A}$ be summable. Then the space $\mathcal{H}$ has a unique reproducing kernel $K_{\mathcal{H}} : \left(\left]-\frac{r}{\beta},\frac{r}{\beta}\right[\times \Omega_r\right) \times \left(\left]-\frac{r}{\beta},\frac{r}{\beta}\right[\times \Omega_r\right) \to \mathbb{R}$ satisfying*

(i) $K_{\mathcal{H}}((t,x),\cdot)$, $K_{\mathcal{H}}(\cdot,(t,x)) \in \mathcal{H}$ for all $(t,x) \in \left]-\frac{r}{\beta},\frac{r}{\beta}\right[\times\Omega_r$,

(ii) $(F, K_{\mathcal{H}}((t,x),\cdot))_{\mathcal{H}} = (F, K_{\mathcal{H}}(\cdot,(t,x)))_{\mathcal{H}} = F(t,x)$ for all $F \in \mathcal{H}$ and $(t,x) \in \left]-\frac{r}{\beta},\frac{r}{\beta}\right[\times\Omega_r$.

This kernel is given by

$$K_{\mathcal{H}}((t,x),(s,y)) = \sum_{n\in\mathcal{N}}\sum_{j=1}^{2n+1}\sum_{i=1}^{2} A_n^{-2}\,\overline{U_{n,j}^{(i)}(t,x)}\,U_{n,j}^{(i)}(s,y) \tag{3}$$

$$= \sum_{n\in\mathcal{N}} A_n^{-2}\,\frac{2n+1}{4\pi}P_n(\xi\cdot\eta)\frac{1}{r^2}\left[\left(\left(\frac{n+1}{2n+1}\right)^2\frac{2}{2n+3}+\left(\frac{n}{2n+1}\right)^2\frac{2}{2n-1}\right)^{-1}\left(\frac{\alpha}{r}\right)^3 ts\right.$$

$$\left.\times P_n\left(-\frac{\alpha}{r}t\right)P_n\left(-\frac{\alpha}{r}s\right)\chi_{\left]-\frac{r}{\alpha},\frac{r}{\alpha}\right[}(t)\,\chi_{\left]-\frac{r}{\alpha},\frac{r}{\alpha}\right[}(s)+\frac{1}{2}(2n+1)\,\frac{\beta}{r}\,P_n\left(-\frac{\beta}{r}t\right)P_n\left(-\frac{\beta}{r}s\right)\right],$$

$t,s\in\left]-\frac{r}{\beta},\frac{r}{\beta}\right[$, $x=r\xi, y=r\eta\in\Omega_r$.

Proof. From the Sobolev Lemma we see that the evaluation functional

$$\begin{array}{rccc} L_{(t,x)}: & \mathcal{H} & \to & \mathbb{C} \\ & F & \mapsto & F(t,x) \end{array}$$

is bounded. From Aronszajn's Theorem it is known that this is equivalent to the existence of a reproducing kernel, which is automatically unique. From the theory of reproducing kernels it is also known that the kernel can be written as in (3) if a countable orthonormal basis is known. For further details we refer to [1, 6]. ∎

Note that $K_{\mathcal{H}}$ is real–valued and $K_{\mathcal{H}}\left((t,x),(s,y)\right) = K_{\mathcal{H}}\left((s,y),(t,x)\right)$.

5 Examples of Reproducing Kernels

We will now give three examples of reproducing kernels $K_{\mathcal{H}}$. As before, $\mathcal{H}$ denotes the space $\mathcal{H}\big(\{A_n\};\left]-\frac{r}{\beta},\frac{r}{\beta}\right[\times\Omega_r\big)$, hence we will choose certain sequences $\{A_n\}_{n\in\mathbb{N}_0}\in\mathcal{A}$ to see what $K_{\mathcal{H}}$ looks like in these special cases.

5.1 Cubic Polynomial Kernel

Let $\{A_n\}\in\mathcal{A}$ be defined by

$$A_n := \begin{cases} \left(1-\frac{n}{N}\right)^{-1}\left(1+2\,\frac{n}{N}\right)^{-1/2} & ,\ n<N \\ 0 & ,\ n\geq N \end{cases},$$

where $N\in\mathbb{N}_0$ can be chosen arbitrarily. Thus, $\mathcal{N}=\{n\in\mathbb{N}_0\mid n<N\}$, $A_n^{-2}=\left(1-\frac{n}{N}\right)^2\left(1+2\,\frac{n}{N}\right)$ for $n\in\mathcal{N}$ and $\{A_n\}$ is summable since $\sum(\{A_n\})$ is a finite sum.

5.2 Abel–Poisson Kernel

Let $\{A_n\}\in\mathcal{A}$ be defined by $A_n := h^{-n/2}$, $h\in]0,1[$, for all $n\in\mathbb{N}_0$, i.e. $\mathcal{N}=\mathbb{N}_0$. Then $\{A_n\}$ is summable since

$$\sum_{n\in\mathbb{N}_0} n^2 A_n^{-2} = \sum_{n\in\mathbb{N}_0} n^2 h^n < +\infty\ .$$

5.3 Truncated Abel–Poisson Kernel

Let $\{A_n\} \in \mathcal{A}$ be defined by

$$A_n := \begin{cases} h^{-n/2} & , \ n \leq N \\ 0 & , \ n > N \end{cases} ,$$

where $h \in]0,1[$ and $N \in \mathbb{N}_0$. Here, $\mathcal{N} = \{n \in \mathbb{N}_0 \mid n \leq N\}$ and $\{A_n\}$ is summable. In the following, we will always choose $h = 1 - 2^{-J}$ and $N = 2 \cdot 2^J$ with $J \in \mathbb{R}^+$ such that $\{A_n\}$ only depends on J.

Figure 1 shows the truncated Abel–Poisson kernel (AP–kernel) for $J = 3$ and $J = 4.5$. $K_{\mathcal{H}}$ has been continuously extended to $[-R/\alpha, R/\alpha]$ from inside the interval, where $r = R$ is here the Earth's radius, $R = 6371$ km, and $\alpha = 5.8$ km/s. Note the increasing time and space localising character of the kernel as the parameter J increases.
For $s = -R/\alpha$ we have a high peak at the same time $t = -R/\alpha$ and the same position ($\xi \cdot \eta = 1$). Hence, the kernel concentrates on the effects near the observed position during a small time window. We can think of a wave travelling through a ball of radius R. At the end of the time interval ($t = R/\alpha$), the waves are focussed at the antipode ($\xi \cdot \eta = -1$). This is an explanation for the peak at the opposite of the diagram. If we choose $s = 0$ we observe a concentration around this time. Finally, at time $s = R/\alpha$ the concentration of the kernel has moved to the time $t = R/\alpha$ for points in the neighbourhood ($\xi \cdot \eta \approx 1$), whereas a high peak is also found for the origin of the motion ($t = -R/\alpha$) at the antipode ($\xi \cdot \eta \approx -1$).

6 Cauchy–Navier Splines

Each modelling process interpreting a real situation handles sets of discrete data, consisting of position, time and corresponding value. Often it is necessary to interpolate this data to obtain results at intermediate positions. Here, the solution of the interpolation problem is determined in a particular finite–dimensional spline space. The terminology "spline" is in accordance with the fact that the interpolant minimises some norm which may be interpreted as an energy norm. Hence, it minimises something like a bending energy as known from one–dimensional cubic spline interpolation.
Similar definitions and results can be found in [12] where the Laplace equation is considered instead of the Cauchy–Navier equation.

Let $\{A_n\} \in \mathcal{A}$ be a summable sequence corresponding to the Sobolev space

$$\mathcal{H} := \mathcal{H}\big(\{A_n\}; \,]-\frac{r}{\beta}, \frac{r}{\beta}[\times \Omega_r\big) ,$$

possessing the reproducing kernel $K_{\mathcal{H}}$. Let further N data points $((t_1, x_1), y_1), \ldots, ((t_N, x_N), y_N) \in \Big(\,]-\frac{r}{\beta}, \frac{r}{\beta}[\times \Omega_r\Big) \times \mathbb{R}$ be given, corresponding to a system $X_N = \{(t_1, x_1), \ldots, (t_N, x_N)\} \subset \,]-\frac{r}{\beta}, \frac{r}{\beta}[\times \Omega_r$ with $(t_i, x_i) \neq (t_k, x_k)$ for $i \neq k$. Let $\mathcal{I}_N(y)$ be the space of all functions $F \in \mathcal{H}$ fulfilling the interpolation condition $F(t_i, x_i) = y_i$ for $i = 1, \ldots, N$, i.e. let

$$\mathcal{I}_N(y) = \{F \in \mathcal{H} \mid F(t_i, x_i) = y_i \,, \ i = 1, \ldots, N\} .$$

Then we can consider the interpolation problem of finding the $\mathcal{H}$–smallest norm interpolant to the prescribed data, i.e.

$$\inf_{F \in \mathcal{I}_N(y)} \|F\|_{\mathcal{H}} .$$

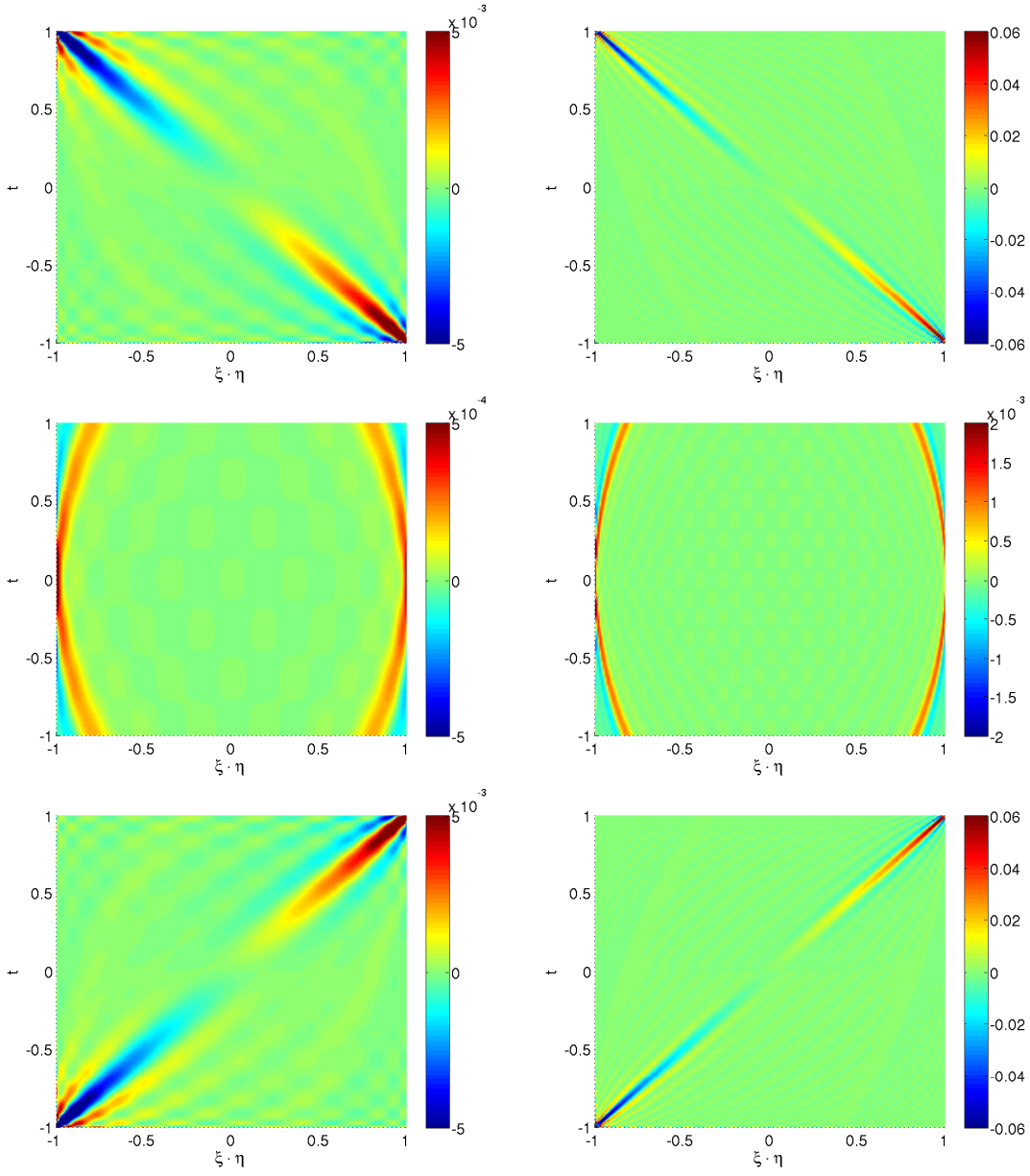

Figure 1: AP–kernel $K_{\mathcal{H}}\left((t, r\xi), (s, r\eta)\right)$ for $s = -r/\alpha$, 0, r/α (top to bottom) with $J = 3$ (left) and $J = 4.5$ (right). The vertical axis refers to $\alpha/r \cdot t$.

Let us start with the following definition of splines in $\mathcal{H}$. We will call them Cauchy–Navier splines, since the derivation of their basis functions $U_{n,j}^{(i)}$, $n \in \mathbb{N}_0\,, j = 1, \ldots, 2n+1\,, i = 1, 2\,,$ is based on the Cauchy–Navier equation. Note that in [4] and [22] Cauchy–Navier splines without time–dependence are developed.

Definition 8 *Any function $S \in \mathcal{H}$ of the form*

$$S(s,y) = \sum_{i=1}^{N} a_i K_{\mathcal{H}}((t_i, x_i), (s,y))\,, \quad a_i \in \mathbb{R}\,,\ (s,y) \in \left]-\frac{r}{\beta}, \frac{r}{\beta}\right[\times \Omega_r\,,$$

is called a Cauchy–Navier spline in $\mathcal{H}$ relative to $X_N = \{(t_1, x_1), \ldots, (t_N, x_N)\}$ in $\left]-\frac{r}{\beta}, \frac{r}{\beta}\right[\times \Omega_r$. The set of all Cauchy–Navier splines is denoted by $\mathrm{Spline}_{\mathrm{CN}}(\{A_n\}; X_N)$.

For later conclusions we need the following lemma.

Lemma 9 *If $F \in \mathcal{H}$ and $S \in \mathrm{Spline}_{\mathrm{CN}}(\{A_n\}; X_N)$ is of the form*

$$S = \sum_{i=1}^{N} a_i K_{\mathcal{H}}((t_i, x_i), \cdot)\,,$$

then

$$(F, S)_{\mathcal{H}} = \sum_{i=1}^{N} a_i F(t_i, x_i)\ .$$

Proof. Due to the reproducing kernel structure of $K_{\mathcal{H}}(\cdot,\cdot)$ in $\mathcal{H}$ we obtain

$$(F, S)_{\mathcal{H}} = \sum_{i=1}^{N} a_i \left(F, K_{\mathcal{H}}((t_i, x_i), \cdot)\right)_{\mathcal{H}} = \sum_{i=1}^{N} a_i F(t_i, x_i)\ .$$

■

Theorem 10 (uniqueness of interpolation) *Let $((t_i, x_i), y_i) \in \left(\left]-\frac{r}{\beta}, \frac{r}{\beta}\right[\times \Omega_r\right) \times \mathbb{R}\,,\ i = 1, \ldots, N$, be N given data points corresponding to $X_N \subset \left]-\frac{r}{\beta}, \frac{r}{\beta}\right[\times \Omega_r$, with the property that $K((t_i, x_i), \cdot)\,,\ i = 1, \ldots, N$, are linearly independent in $\mathcal{H}$. Then there exists a unique $S \in \mathrm{Spline}_{\mathrm{CN}}(\{A_n\}; X_N) \cap \mathcal{I}_N(y)$, denoted by S_N.*

Proof. As a spline, $S \in \mathrm{Spline}_{\mathrm{CN}}(\{A_n\}; X_N)$ contains N unknown coefficients a_i:

$$S(s,y) = \sum_{i=1}^{N} a_i K_{\mathcal{H}}((t_i, x_i), (s,y))\,, \quad (s,y) \in \left]-\frac{r}{\beta}, \frac{r}{\beta}\right[\times \Omega_r\,.$$

Since S is an element of $\mathcal{I}_N(y)$ we receive a system of linear equations

$$\sum_{i=1}^{N} a_i K_{\mathcal{H}}((t_i, x_i), (t_k, x_k)) = y_k\ ,\ k = 1, \ldots, N\,.$$

The coefficient matrix with the entries

$$K_{\mathcal{H}}((t_i, x_i), (t_k, x_k)) = (K_{\mathcal{H}}((t_i, x_i), \cdot), K_{\mathcal{H}}((t_k, x_k), \cdot))_{\mathcal{H}}\ ,\ i, k = 1, \ldots, N\,,$$

is a Gram matrix. As the nodal points $(t_i, x_i) \in \left]-\frac{r}{\beta}, \frac{r}{\beta}\right[\times \Omega_r$, $i = 1, \ldots, N$, have been chosen such that $K_{\mathcal{H}}((t_i, x_i), \cdot)$ are linearly independent in $\mathcal{H}$, the Gram matrix is positive definite and the system is uniquely solvable. ∎

Since we are interested in having unique solutions, we will from now on assume that $X_N \subset \left]-\frac{r}{\beta}, \frac{r}{\beta}\right[\times \Omega_r$ is chosen such that $K_{\mathcal{H}}((t_i, x_i), \cdot)\,,\ i = 1, \ldots, N$, are linearly independent in $\mathcal{H}$.
In the following, we will prove some important properties of our solution S_N in analogy to [12].

Theorem 11 (first minimum property) *Let $F \in \mathcal{I}_N(y)$. Then*

$$\|F\|_{\mathcal{H}}^2 = \|S_N\|_{\mathcal{H}}^2 + \|S_N - F\|_{\mathcal{H}}^2 \ .$$

Proof. From Lemma 9 we have

$$(S_N - F, S_N)_{\mathcal{H}} = 0\,.$$

Consequently,

$$\begin{aligned} \|F\|_{\mathcal{H}}^2 &= (F, F)_{\mathcal{H}} = (S_N - (S_N - F), S_N - (S_N - F))_{\mathcal{H}} \\ &= (S_N, S_N)_{\mathcal{H}} - 2\,\mathrm{Re}\,(S_N - F, S_N)_{\mathcal{H}} + (S_N - F, S_N - F)_{\mathcal{H}} \\ &= \|S_N\|_{\mathcal{H}}^2 + \|S_N - F\|_{\mathcal{H}}^2\,. \end{aligned}$$

∎

Theorem 11 says that among all interpolating functions in $\mathcal{H}$ there is one and only one function with minimal Sobolev norm $\|\cdot\|_{\mathcal{H}}$. The minimising function is the unique interpolating spline S_N. This property is the justification of the name "spline".

Theorem 12 (second minimum property) *Let $F \in \mathcal{I}_N(y)$ and $S \in \mathrm{Spline}_{\mathrm{CN}}(\{A_n\}; X_N)$. Then*

$$\|S - F\|_{\mathcal{H}}^2 = \|S_N - F\|_{\mathcal{H}}^2 + \|S - S_N\|_{\mathcal{H}}^2 \ .$$

Proof. With Lemma 9 we find

$$(S_N - F, S - S_N)_{\mathcal{H}} = (S_N - F, S)_{\mathcal{H}} - (S_N - F, S_N)_{\mathcal{H}} = 0\,.$$

Hence,

$$\begin{aligned} \|S - F\|_{\mathcal{H}}^2 &= \|S - S_N + S_N - F\|_{\mathcal{H}}^2 \\ &= (S - S_N + S_N - F, S - S_N + S_N - F)_{\mathcal{H}} \\ &= (S - S_N, S - S_N)_{\mathcal{H}} + 2\,\mathrm{Re}\,(S_N - F, S - S_N)_{\mathcal{H}} + (S_N - F, S_N - F)_{\mathcal{H}} \\ &= \|S - S_N\|_{\mathcal{H}}^2 + \|S_N - F\|_{\mathcal{H}}^2\,. \end{aligned}$$

∎

Theorem 12 tells us that in the space $\mathrm{Spline}_{\mathrm{CN}}(\{A_n\}; X_N)$ of all splines in $\mathcal{H}$ relative to X_N, there is one and only one spline S_N which is closest (in the $\|\cdot\|_{\mathcal{H}}$–sense) to a given function F. This so–called best approximation is the spline which is given by the interpolation conditions $S(t_i, x_i) = F(t_i, x_i) = y_i\,,\ i = 1, \ldots, N$.

In the following, we will derive an error estimate and a convergence proof based on a kind of Lipschitz continuity of the reproducing kernels. Since the numerical calculations presented here are restricted to the smaller time interval $]-r/\alpha, r/\alpha[$ we will also only restrict our considerations to this subinterval. We start with the following lemma.

Lemma 13 *Let $\{A_n\}$ be chosen such that*

$$\sum_{n\in\mathcal{N}} A_n^{-2} n^4 < +\infty \ .$$

Then there exists a constant $C(\{A_n\})$ such that

$$|K_{\mathcal{H}}((t,x),(s,y)) - K_{\mathcal{H}}((t,x),(u,z))| \leq C(\{A_n\}) \left(\left| \frac{y}{r} - \frac{z}{r} \right| + |s-u| \right)$$

for all $s,t,u \in]-r/\alpha, r/\alpha[$ and all $x,y,z \in \Omega_r$.

Proof. We use the representations $x = r\xi$, $y = r\eta$, and $z = r\zeta$ and the abbreviation

$$\gamma_n := \left(\left(\frac{n+1}{2n+1} \right)^2 \frac{2}{2n+3} + \left(\frac{n}{2n+1} \right)^2 \frac{2}{2n-1} \right)^{-1} \left(\frac{\alpha}{r} \right)^3 .$$

Note that $\gamma_n = \mathrm{O}(n)$ as $n \to \infty$. Using the derived formula for the reproducing kernel we obtain

$$\begin{aligned}
&|K_{\mathcal{H}}((t,x),(s,y)) - K_{\mathcal{H}}((t,x),(u,z))| \\
&= \left| \sum_{n\in\mathcal{N}} A_n^{-2} \frac{2n+1}{4\pi r^2} \left(\gamma_n t P_n\left(-\frac{\alpha}{r}\, t\right) \left(P_n(\xi\cdot\eta) s P_n\left(-\frac{\alpha}{r}\, s\right) - P_n(\xi\cdot\zeta) u P_n\left(-\frac{\alpha}{r}\, u\right) \right) \right.\right. \\
&\qquad \left.\left. + \frac{1}{2}(2n+1)\frac{\beta}{r} P_n\left(-\frac{\beta}{r}\, t\right) \left(P_n(\xi\cdot\eta) P_n\left(-\frac{\beta}{r}\, s\right) - P_n(\xi\cdot\zeta) P_n\left(-\frac{\beta}{r}\, u\right) \right) \right) \right| \\
&\leq \sum_{n\in\mathcal{N}} A_n^{-2} \frac{2n+1}{4\pi r^2}\, \gamma_n \frac{r}{\alpha} \left(\left| P_n(\xi\cdot\eta) s P_n\left(-\frac{\alpha}{r}\, s\right) - P_n(\xi\cdot\zeta) s P_n\left(-\frac{\alpha}{r}\, s\right) \right| \right. \\
&\qquad \left. + \left| P_n(\xi\cdot\zeta) s P_n\left(-\frac{\alpha}{r}\, s\right) - P_n(\xi\cdot\zeta) u P_n\left(-\frac{\alpha}{r}\, u\right) \right| \right) \\
&\quad + \sum_{n\in\mathcal{N}} A_n^{-2} \frac{2n+1}{4\pi r^2}\, \frac{1}{2}\, (2n+1)\frac{\beta}{r} \left(\left| P_n(\xi\cdot\eta) P_n\left(-\frac{\beta}{r}\, s\right) - P_n(\xi\cdot\zeta) P_n\left(-\frac{\beta}{r}\, s\right) \right| \right. \\
&\qquad \left. + \left| P_n(\xi\cdot\zeta) P_n\left(-\frac{\beta}{r}\, s\right) - P_n(\xi\cdot\zeta) P_n\left(-\frac{\beta}{r}\, u\right) \right| \right) \qquad (4)
\end{aligned}$$

where we used that $|P_n(w)| \leq 1$ for all $n \in \mathbb{N}_0$ and all $w \in [-1,1]$. The mean value theorem of differentiation now implies the existence of constants $\tau \in]-1,1[$ and $\varrho_j \in]-r/\alpha, r/\alpha[$ such that

$$\begin{aligned}
&|K_{\mathcal{H}}((t,x),(s,y)) - K_{\mathcal{H}}((t,x),(u,z))| \\
&\leq \sum_{n\in\mathcal{N}} A_n^{-2} \frac{2n+1}{4\pi r^2}\, \gamma_n \frac{r}{\alpha} \left(|P_n'(\tau)|\, |\xi\cdot\eta - \xi\cdot\zeta| \left| s P_n\left(-\frac{\alpha}{r}\, s\right) \right| \right. \\
&\qquad \left. + |P_n(\xi\cdot\zeta)| \left| P_n\left(-\frac{\alpha}{r}\, \varrho_1\right) + \varrho_1 \left(-\frac{\alpha}{r}\right) P_n'\left(-\frac{\alpha}{r}\, \varrho_1\right) \right| |s-u| \right) \\
&\quad + \sum_{n\in\mathcal{N}} A_n^{-2} \frac{(2n+1)^2}{8\pi r^2}\, \frac{\beta}{r} \left(|P_n'(\tau)|\, |\xi\cdot\eta - \xi\cdot\zeta| \left| P_n\left(-\frac{\beta}{r}\, s\right) \right| \right. \\
&\qquad \left. + |P_n(\xi\cdot\zeta)| \frac{\beta}{r} \left| P_n'\left(-\frac{\beta}{r}\, \varrho_2\right) \right| |s-u| \right)
\end{aligned}$$

$$
\begin{aligned}
&\leq \sum_{n\in\mathcal{N}} A_n^{-2}\,\frac{2n+1}{4\pi r^2}\,\gamma_n\,\frac{r}{\alpha}\left(\frac{n(n+1)}{2}\,|\xi\cdot(\eta-\zeta)|\,\frac{r}{\alpha}+\left(1+\frac{n(n+1)}{2}\right)\,|s-u|\right)\\
&\quad+\sum_{n\in\mathcal{N}} A_n^{-2}\,\frac{(2n+1)^2}{8\pi r^2}\,\frac{\beta}{r}\left(\frac{n(n+1)}{2}\,|\xi\cdot(\eta-\zeta)|+\frac{\beta}{r}\,\frac{n(n+1)}{2}\,|s-u|\right)\\
&\leq \left(\sum_{n\in\mathcal{N}} A_n^{-2}\,\frac{2n+1}{4\pi r^2}\,\gamma_n\,\frac{r}{\alpha}\max\left(\frac{r}{\alpha}\,\frac{n(n+1)}{2},1+\frac{n(n+1)}{2}\right)\right)(|\eta-\zeta|+|s-u|)\\
&\quad+\left(\sum_{n\in\mathcal{N}} A_n^{-2}\,\frac{(2n+1)^2}{8\pi r^2}\,\frac{\beta}{r}\max\left(1,\frac{\beta}{r}\right)\frac{n(n+1)}{2}\right)(|\eta-\zeta|+|s-u|) \qquad (5)
\end{aligned}
$$

since $|P_n'(w)|\leq P_n'(1)=n(n+1)/2$ for all $w\in[-1,1]$ and all $n\in\mathbb{N}_0$ (see, for example, [17]). ∎

For formulating an error estimate we need a tool to measure gaps in the point grid.

Definition 14 *Let $X_N=\{(t_j,x_j)\}_{j=1,\ldots,N}$ be a given set of mutually distinct pairs $(t_j,x_j)\in\,]-r/\alpha,r/\alpha[\times\Omega_r$. Then we define the width of this grid by*

$$\Theta_{X_N}:=\max_{(s,y)\in]-r/\alpha,r/\alpha[\times\Omega_r}\ \min_{(t,x)\in X_N}\left(\left|\frac{y}{r}-\frac{x}{r}\right|+|s-t|\right).$$

Θ_{X_N} measures a kind of radius of the largest gap in the spatio–temporal point grid. We can now derive a convergence result in correspondence to a result for the Laplace equation in [12].

Theorem 15 *Let $F\in\mathcal{H}\big(\{A_n\};\,]-\frac{r}{\beta},\frac{r}{\beta}[\,\times\Omega_r\big)$ where $\{A_n\}$ satisfies*

$$\sum_{n=0}^{\infty} A_n^{-2}n^4<+\infty\ .$$

Moreover, let $X_N=\{(t_j^{(N)},x_j^{(N)})\}_{j=1,\ldots,N}$ be a set of N time–space–pairs for each $N\in\mathbb{N}$ such that for every $N\in\mathbb{N}$ the N functions $\{K_{\mathcal{H}}(t,x)\}_{(t,x)\in X_N}$ are linearly independent. If (S_N) is the sequence of splines which are determined uniquely by

$$
\begin{aligned}
S_N &\in \mathrm{Spline}_{\mathrm{CN}}(\{A_n\};X_N)\\
S_N\left(t_j^{(N)},x_j^{(N)}\right) &= F\left(t_j^{(N)},x_j^{(N)}\right)\quad \textit{for all } j=1,\ldots,N\,, \qquad (6)
\end{aligned}
$$

then there exists a constant $\tilde{C}(\{A_n\})$, independent of F, such that

$$\max_{(t,x)\in]-r/\alpha,r/\alpha[\times\Omega_r}|S_N(t,x)-F(t,x)|\leq\tilde{C}(\{A_n\})\Theta_{X_N}^{1/2}\,\|F\|_{\mathcal{H}}\ .$$

In particular, if $\lim_{N\to\infty}\Theta_{X_N}=0$ then

$$\lim_{N\to\infty}\ \max_{(t,x)\in]-r/\alpha,r/\alpha[\times\Omega_r}|S_N(t,x)-F(t,x)|=0\ .$$

Proof. Let $N\in\mathbb{N}$ and $(t,x)\in]-r/\alpha,r/\alpha[\times\Omega_r$ be fixed. For this pair there exists $(t_j^{(N)},x_j^{(N)})\in X_N$ such that

$$r^{-1}\left|x-x_j^{(N)}\right|+\left|t-t_j^{(N)}\right|\leq\Theta_{X_N}\ .$$

One can now derive due to Equation (6), the property of a reproducing kernel, Theorem 11, and the Cauchy–Schwarz inequality that

$$
\begin{aligned}
|S_N(t,x) - F(t,x)| &\leq \left|S_N(t,x) - S_N\left(t_j^{(N)}, x_j^{(N)}\right) + S_N\left(t_j^{(N)}, x_j^{(N)}\right) - F(t,x)\right| \qquad (7)\\
&= \left|S_N(t,x) - S_N\left(t_j^{(N)}, x_j^{(N)}\right) + F\left(t_j^{(N)}, x_j^{(N)}\right) - F(t,x)\right| \\
&= \left|\left(K_{\mathcal{H}}((t,x),\cdot) - K_{\mathcal{H}}\left(\left(t_j^{(N)}, x_j^{(N)}\right),\cdot\right), S_N - F\right)_{\mathcal{H}}\right| \\
&\leq \left(K_{\mathcal{H}}((t,x),\cdot) - K_{\mathcal{H}}\left(\left(t_j^{(N)}, x_j^{(N)}\right),\cdot\right), K_{\mathcal{H}}((t,x),\cdot) - K_{\mathcal{H}}\left(\left(t_j^{(N)}, x_j^{(N)}\right),\cdot\right)\right)_{\mathcal{H}}^{1/2} \\
&\quad \times \left(\|S_N\|_{\mathcal{H}} + \|F\|_{\mathcal{H}}\right) \\
&\leq \left(K_{\mathcal{H}}((t,x),(t,x)) + K_{\mathcal{H}}\left(\left(t_j^{(N)}, x_j^{(N)}\right), \left(t_j^{(N)}, x_j^{(N)}\right)\right) - 2K_{\mathcal{H}}\left(\left(t_j^{(N)}, x_j^{(N)}\right), (t,x)\right)\right)^{1/2} \\
&\quad \times 2\,\|F\|_{\mathcal{H}}\ .
\end{aligned}
$$

Using Lemma 13 and the symmetry of the reproducing kernel we obtain

$$
\left|K_{\mathcal{H}}((t,x),(t,x)) - K_{\mathcal{H}}\left(\left(t_j^{(N)}, x_j^{(N)}\right),(t,x)\right)\right| \leq C(\{A_n\})\left(r^{-1}\left|x - x_j^{(N)}\right| + \left|t - t_j^{(N)}\right|\right)
$$

and

$$
\begin{aligned}
&\left|K_{\mathcal{H}}\left(\left(t_j^{(N)}, x_j^{(N)}\right), \left(t_j^{(N)}, x_j^{(N)}\right)\right) - K_{\mathcal{H}}\left(\left(t_j^{(N)}, x_j^{(N)}\right),(t,x)\right)\right| \\
&\quad \leq C(\{A_n\})\left(r^{-1}\left|x - x_j^{(N)}\right| + \left|t - t_j^{(N)}\right|\right)
\end{aligned}
$$

such that, finally,

$$
|S_N(t,x) - F(t,x)| \leq 2(2C(\{A_n\}))^{1/2}\Theta_{X_N}^{1/2}\|F\|_{\mathcal{H}}\ .
$$

■

7 Numerical Results

In this chapter we will apply the Cauchy–Navier splines developed in the previous chapter to artificial earthquake data and present the numerical results of our computations. Earthquake data is usually given at fixed gauging stations on the Earth's surface at certain times. Section 7.1 is dedicated to test our method with a synthetic wave function known at any time everywhere on the Earth. In Section 7.2 we will use synthetic earthquake data generated by the program GEMINI (see [5]). This program provides us with realistic displacement data. Moreover, we are able to choose the position of the gauging stations ourselves, which is advantageous for numerical tests. The gained experiences could then be used for further research into real earthquakes.

Since we want to study the Earth's surface, R will from now on always denote the Earth's radius, $R = 6371$ km. The Earth's surface is approximated by the sphere Ω_R. $\alpha = 5.8$ km/s and $\beta = 3.2$ km/s are the velocities of compressional and shear body waves, respectively.
For numerical purposes we will restrict our attention to $]-r/\alpha, r/\alpha[$ since all basis functions differ from zero almost everywhere in this subinterval.

7.1 Synthetic Waves

For our first numerical tests we consider a simple synthetic wave function in form of two Gaussians which move through the Earth with different velocities. Therefore, we define $\tilde{W} : \left]0\,, 2\,\frac{R}{\alpha}\right[\times \Omega_R \to \mathbb{R}$ in the following way:

$$\tilde{W}(s,x) = \frac{\exp\left(-\gamma\left(-|x-y| + \alpha s + \delta\right)^2\right) + \exp\left(-\gamma\left(-|x-y| + \beta s + \delta\right)^2\right)}{|x-y|}\ , \tag{8}$$

$s \in \left]0\,, 2\,\frac{R}{\alpha}\right[$, $x \in \Omega_R$, where $y \in \overline{\Omega_R^{\text{int}}}$ denotes the focus, $\gamma, \delta \in \mathbb{R}$ are parameters and $\alpha, \beta \in \mathbb{R}$ the velocities of the waves. We choose here the hypocentre to be located $1‰\, R$ under the north pole, i.e. $y = (0, 0, R - 0.001R)^{\mathrm{T}}$, and $\gamma = 50$, $\delta = 0$, $\alpha = 5.8$ and $\beta = 3.2$. Since we want the earthquake to start at $t = -R/\alpha$ we set $s(t) := t + R/\alpha$ with $t \in \left]-\frac{R}{\alpha}, \frac{R}{\alpha}\right[$ and consider $W(t,x) := \tilde{W}(s(t), x)$. W is a wave that propagates through the whole Earth but is only sampled at the surface. Figure 2 illustrates the real wave function $W(t,x)$ for $\varphi(x), \vartheta(x) \in \left[0, \frac{\pi}{2}\right]$ and some fixed times $t \in \left]-\frac{R}{\alpha}, \frac{R}{\alpha}\right[$. For better comparability of the pictures among each other and especially with corresponding subsequent results the colourbars are adjusted. The maximal values of W can be found in Table 1.

Our intention is to reconstruct the wave W from given values on a point grid in $\left]-\frac{R}{\alpha}, \frac{R}{\alpha}\right[\times \Omega_R$ by spline approximation in $\mathcal{H}$. Thus, we start our considerations by constructing a point grid $\{(t_1, x_1), \ldots, (t_N, x_N)\} \subset \left]-\frac{R}{\alpha}, \frac{R}{\alpha}\right[\times \Omega_R$. Then we calculate observables $y_k := W(t_k, x_k)$, $k = 1, \ldots, N$ for the point grid and finally solve the linear equation system

$$\sum_{i=1}^{N} a_i K_{ik} = y_k\ ,\ k = 1, \ldots, N\,,$$

where

$$K = \left(K_{\mathcal{H}}((t_i, x_i), (t_k, x_k))\right)_{i,k=1,\ldots,N}\ .$$

When we try to solve this system numerically we observe that the matrix K is very ill–conditioned. As a method of regularisation, the condition can be improved by weighting the main diagonal.

Theorem 16 *Let $\lambda > 0$, $y_i \in \mathbb{R}$ and $\gamma_i := K_{\mathcal{H}}((t_i, x_i), (t_i, x_i)) \neq 0\,,\ i = 1, \ldots, N$. The matrix*

$$K' := \left(K_{\mathcal{H}}((t_i, x_i), (t_k, x_k))\right)_{i,k=1,\ldots,N} + \lambda\ \left(K_{\mathcal{H}}((t_i, x_i), (t_k, x_k))\,\delta_{ik}\right)_{i,k=1,\ldots,N}$$

is assumed to be non–singular. Then the function $S \in \mathcal{H}$ of the form

$$S(t,x) = \sum_{i=1}^{N} a_i K_{\mathcal{H}}((t_i, x_i), (t, x))\ ,\quad (t,x) \in \left]-\frac{r}{\alpha}, \frac{r}{\alpha}\right[\times \Omega_r\ , \tag{9}$$

with coefficients $a_i \in \mathbb{R}$, $i = 1, \ldots, N$, uniquely determined by the linear equations

$$S(t_i, x_i) + \lambda\,\gamma_i\,a_i = y_i\,,\ i = 1, \ldots, N\,, \tag{10}$$

represents the only element of $\mathcal{H}$ satisfying

$$\sum_{i=1}^{N} \frac{\left(S(t_i, x_i) - y_i\right)^2}{\gamma_i} + \lambda\,\|S\|_{\mathcal{H}}^2\ \leq\ \sum_{i=1}^{N} \frac{\left(F(t_i, x_i) - y_i\right)^2}{\gamma_i} + \lambda\,\|F\|_{\mathcal{H}}^2 \tag{11}$$

for all real–valued functions $F \in \mathcal{H}$.

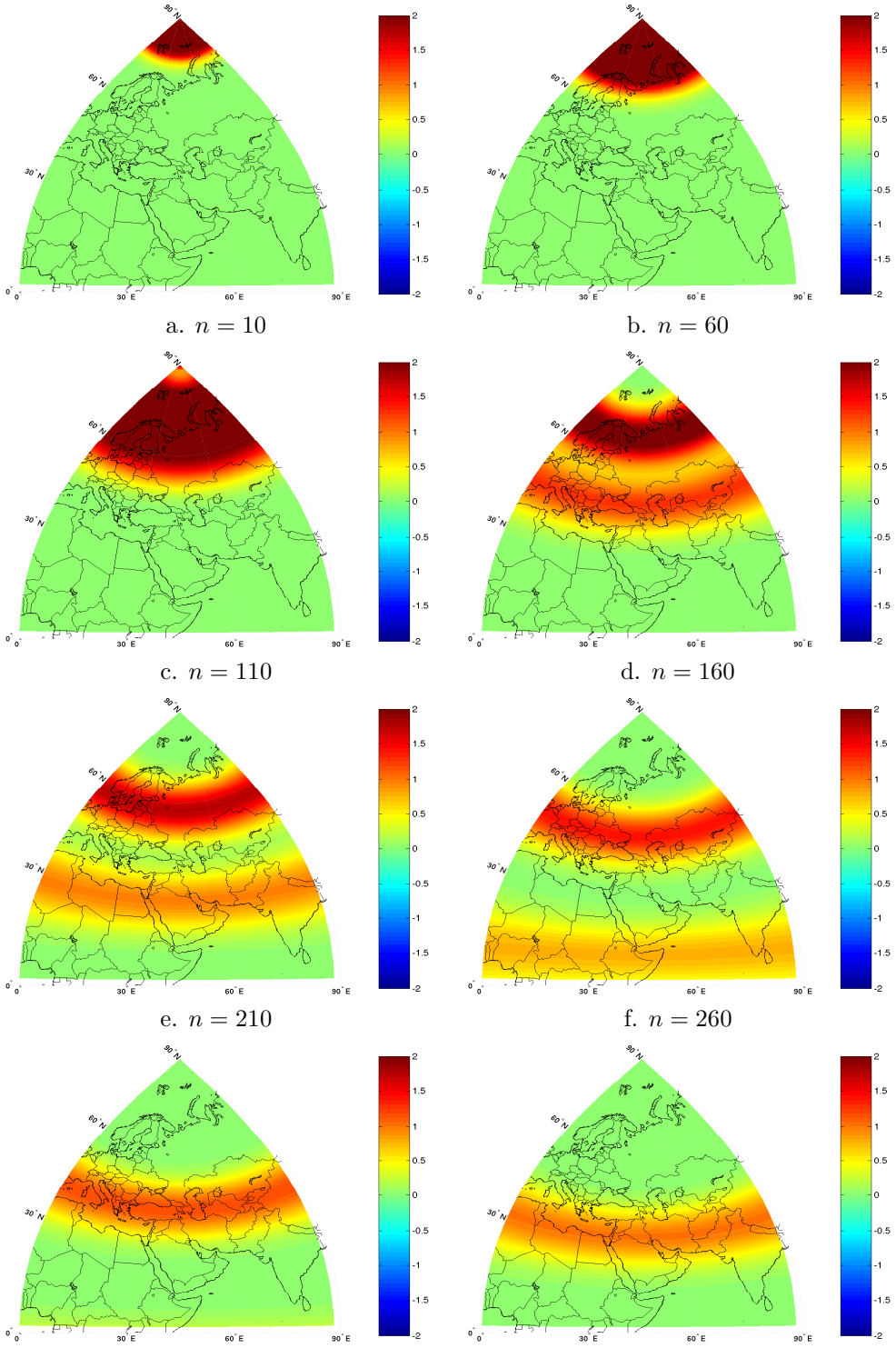

a. $n = 10$ b. $n = 60$

c. $n = 110$ d. $n = 160$

e. $n = 210$ f. $n = 260$

g. $n = 310$ h. $n = 360$

Figure 2: Original wave function W for $t = (-1 + (n-1)\,0.005)\,R/\alpha$.

Proof. Inserting the representation (9) into the equations (10) results in a linear system with the unknowns a_i and the matrix K'. Since K' is assumed to be non–singular, the coefficients are uniquely determined.
Let F be an arbitrary real–valued function in $\mathcal{H}$. Our purpose is to show that the function S determined by condition (10) satisfies the property (11). Solving (10) for a_i, multiplying by $F(t_i, x_i)$, and summing over $i = 1, \ldots, N$ gives

$$\sum_{i=1}^{N} a_i F(t_i, x_i) = \frac{1}{\lambda} \sum_{i=1}^{N} F(t_i, x_i) \, \frac{y_i - S(t_i, x_i)}{\gamma_i} \ .$$

With Lemma 9 we obtain

$$\lambda \, (F, S)_{\mathcal{H}} = \sum_{i=1}^{N} F(t_i, x_i) \, \frac{y_i - S(t_i, x_i)}{\gamma_i} \ . \tag{12}$$

Note that the scalar product $(F, S)_{\mathcal{H}}$ is symmetric due to Lemma 9 since F and S are real–valued functions.
Now an elementary calculation shows us that

$$\begin{aligned}
&\sum_{i=1}^{N} \frac{\left(F(t_i, x_i) - y_i\right)^2}{\gamma_i} + \lambda \, (F, F)_{\mathcal{H}} \\
&\quad = \sum_{i=1}^{N} \frac{\left(S(t_i, x_i) - y_i\right)^2}{\gamma_i} + \lambda \, (S, S)_{\mathcal{H}} + \sum_{i=1}^{N} \frac{\left(F(t_i, x_i) - S(t_i, x_i)\right)^2}{\gamma_i} \\
&\qquad + 2 \sum_{i=1}^{N} \frac{\left(F(t_i, x_i) - S(t_i, x_i)\right) \left(S(t_i, x_i) - y_i\right)}{\gamma_i} + 2 \, \lambda \, (F - S, S)_{\mathcal{H}} + \lambda \, (F - S, F - S)_{\mathcal{H}}
\end{aligned}$$

According to (12) it follows that

$$2 \sum_{i=1}^{N} \frac{\left(F(t_i, x_i) - S(t_i, x_i)\right) \left(S(t_i, x_i) - y_i\right)}{\gamma_i} + 2 \, \lambda \, (F - S, S)_{\mathcal{H}} = 0 \ .$$

Therefore, we have

$$\begin{aligned}
&\sum_{i=1}^{N} \frac{\left(F(t_i, x_i) - y_i\right)^2}{\gamma_i} + \lambda \, \|F\|_{\mathcal{H}}^2 \\
&\quad = \sum_{i=1}^{N} \frac{\left(S(t_i, x_i) - y_i\right)^2}{\gamma_i} + \lambda \, \|S\|_{\mathcal{H}}^2 + \sum_{i=1}^{N} \frac{\left(F(t_i, x_i) - S(t_i, x_i)\right)^2}{\gamma_i} + \lambda \, \|F - S\|_{\mathcal{H}}^2 \ .
\end{aligned} \tag{13}$$

Since

$$\gamma_i = K_{\mathcal{H}}((t_i, x_i), (t_i, x_i)) = (K_{\mathcal{H}}((t_i, x_i), \cdot), K_{\mathcal{H}}((t_i, x_i), \cdot))_{\mathcal{H}} > 0 \ ,$$

(13) implies that

$$\sum_{i=1}^{N} \frac{\left(S(t_i, x_i) - y_i\right)^2}{\gamma_i} + \lambda \, \|S\|_{\mathcal{H}}^2 \ \leq \ \sum_{i=1}^{N} \frac{\left(F(t_i, x_i) - y_i\right)^2}{\gamma_i} + \lambda \, \|F\|_{\mathcal{H}}^2 \ ,$$

where equality holds if and only if $S = F$. ∎

The resulting spline is called smoothing spline. For increasing λ the condition of K' gets better and the spline becomes smoother. However, the larger λ gets, the more our spline may differ from the measurements. Hence, we have to choose the smoothing parameter λ in a way that the equation system is well–conditioned and the resulting spline is close enough to our measurements.

With respect to the time we consider 50 points in the interval $\left]-\frac{R}{\alpha}, \frac{R}{\alpha}\right[\subset \mathbb{R}$. It is well known that, usually, interpolating functions tend to oscillate at the boundaries if one uses equidistant nodes. These oscillations can be reduced by using Chebyshev nodes, which are the roots of the Chebyshev polynomials on $[-1, 1]$ (see e.g. [21]):

$$x_k = \cos\left(\frac{2k-1}{n}\,\frac{\pi}{2}\right) \ , \quad k = 1, \ldots, n \ ,$$

where $n \in \mathbb{N}$ is the degree of the considered polynomial.
Therefore, we use the point grid

$$t_k = x_k \cdot R/\alpha = \cos\left(\frac{2k-1}{50}\,\frac{\pi}{2}\right) \cdot R/\alpha \ , \quad k = 1, \ldots, 50 \ .$$

Moreover, we have to construct a point grid on the spatial domain Ω_R.

Definition 17 *A Reuter grid on the unit sphere, dependent on the choice of a control parameter $\gamma \in \mathbb{N}$, is given by the points $(\varphi_{ij}, \vartheta_i)$ as follows:*

(i) $\vartheta_0 := 0$, $\varphi_{01} := 0$ *(North Pole),*

(ii) $\triangle\vartheta := \pi/\gamma$,

(iii) $\vartheta_i := i\triangle\vartheta \ , \quad 1 \le i \le \gamma - 1$,

(iv) $\gamma_i := \left[2\pi/\arccos\left(\left(\cos\triangle\vartheta - \cos^2\vartheta_i\right)/\sin^2\vartheta_i\right)\right]$, *where the Gauß bracket $[x]$ denotes the largest integer less than or equal to x,*

(v) $\varphi_{ij} := (j - 1/2)(2\pi/\gamma_i) \ , \quad 1 \le j \le \gamma_i$,

(vi) $\vartheta_\gamma := \pi$, $\varphi_{\gamma 1} = 0$ *(South Pole).*

The definition of this and other point grids on the sphere can be found in [12, 18]. The parameter $\gamma + 1$ gives the number of latitudes which are equidistributed. On each latitude, the points are constructed such that two adjacent points have the same spherical distance as two adjacent latitudes. Reuter grids are, therefore, more equidistributed on the sphere than the equiangular grids used above. Here, we set $\gamma = 17$ and select all points with $\varphi, \vartheta \in]0, \frac{\pi}{2}[$. In this manner we obtain 43 points $x(R, \varphi, \vartheta)$ which are displayed in Figure 3.

Numerical tests and comparisons of the splines with the original wave function W show that for this point grid the best results are achieved with a truncated Abel–Poisson kernel ($J = 2.8$) and smoothing parameter $\lambda = 10^{-2.5}$. Figure 4 displays the corresponding spline S and the function W on the whole time interval at one gauging station, $(\varphi, \vartheta) = (0.814, 0.924) \,\hat{=}\, (43.4^\circ$ N, 52.9° E), which is a station in the centre of the observed spatial domain, and at three other points with increasing distance to the station. The distances are chosen smaller than the grid width. Despite of the approximation instead of an interpolation the positions of the wavefront are very well represented.

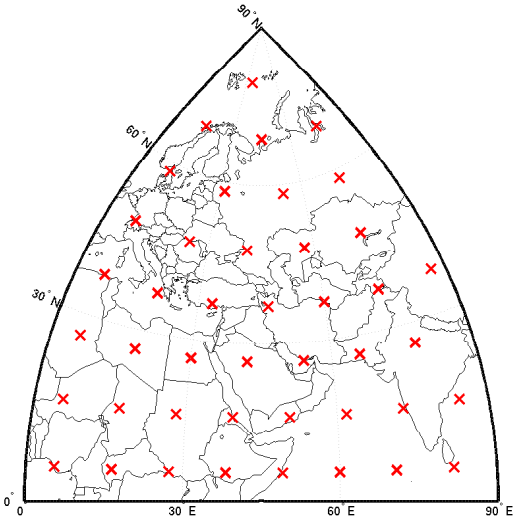

Figure 3: 43 stations on a Reuter grid.

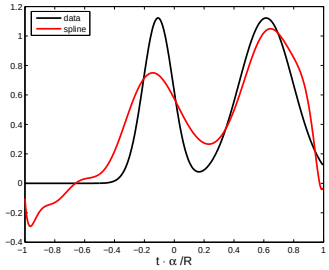

a. $\varphi = \varphi_0 := 0.814$, $\vartheta = \vartheta_0 := 0.924$

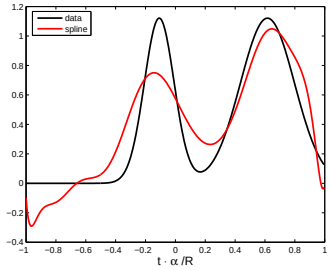

b. $\varphi = \varphi_0 + 0.001$, $\vartheta = \vartheta_0 + 0.001$

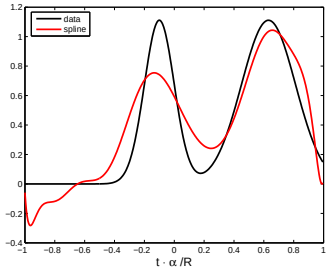

c. $\varphi = \varphi_0 + 0.01$, $\vartheta = \pi/5 + 0.01$

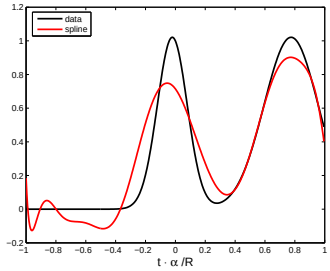

d. $\varphi = \varphi_0 + 0.1$, $\vartheta = \pi/5 + 0.1$

Figure 4: $S(t, x(R, \varphi, \vartheta)$, truncated AP–kernel, $J = 2.8$, $\lambda = 10^{-2.5}$.

To examine the quality of the approximation both at the sampling points and between them we evaluate the spline S on a grid of 1600 points $(t_i, x_j) \in \left]-\frac{R}{\alpha}, \frac{R}{\alpha}\right[\times \Omega_R$, where $x_j \in \Omega_R\,, j = 1, \ldots, 4\,,$ are the 4 points mentioned above and $t_i\,,\ i = 1, \ldots, 400$ are equidistant points in $\left]-\frac{R}{\alpha}, \frac{R}{\alpha}\right[$. Then we compare the values with the wave function W at these points by calculating the rooted mean square error

$$\varepsilon_{\mathrm{rms}} = \sqrt{\frac{1}{1600} \sum_{i=1}^{400} \sum_{j=1}^{4} \left|S(t_i, x_j) - W(t_i, x_j)\right|^2} = 0.1588\ .$$

In Figure 5 we see the spline S on the complete octant at some fixed points $t \in \left]-\frac{R}{\alpha}, \frac{R}{\alpha}\right[$. In comparison to the original wave the only obvious difference is that the first Gaussian is not as distinct. Figure 6 shows the logarithm of the absolute error between the spline and the original wave, i.e. $\log(\,|S(t,x) - W(t,x)|\,)$, confirming that the error is very small. Additionally, we calculate for each point t the rooted mean square error over 2500 spatial grid points:

$$\varepsilon_{\mathrm{rms}}(t) = \sqrt{\frac{1}{2500} \sum_{i=1}^{2500} \left|S(t, x_i) - W(t, x_i)\right|^2}\ .$$

The results are listed in Table 1. We notice that we have very high errors at the beginning of the time interval, but we have to compare these errors to the maximal values of the wave function W. W has a very high peak at the northpole which is not sampled since we have no gauging station near this point. One advantage of the spline method is that such local errors do not spread over the whole domain.

n	10	50	110	160	210	260	310	360
$\varepsilon_{\mathrm{rms}}(t)$	265.79	37.855	1.1753	0.3646	0.1904	0.1837	0.1637	0.2173
$\max_x(W(t))$	1879.7	283.56	11.213	2.3355	1.7615	1.4108	1.1748	1.0097

Table 1: Rooted mean square errors and maximal values of W and S for $t = (-1 + (n - 1)\,0.005)\,R/\alpha$.

From these results we can conclude that the applied method works successfully. Thus, in the following section, we will investigate realistic earthquake data.

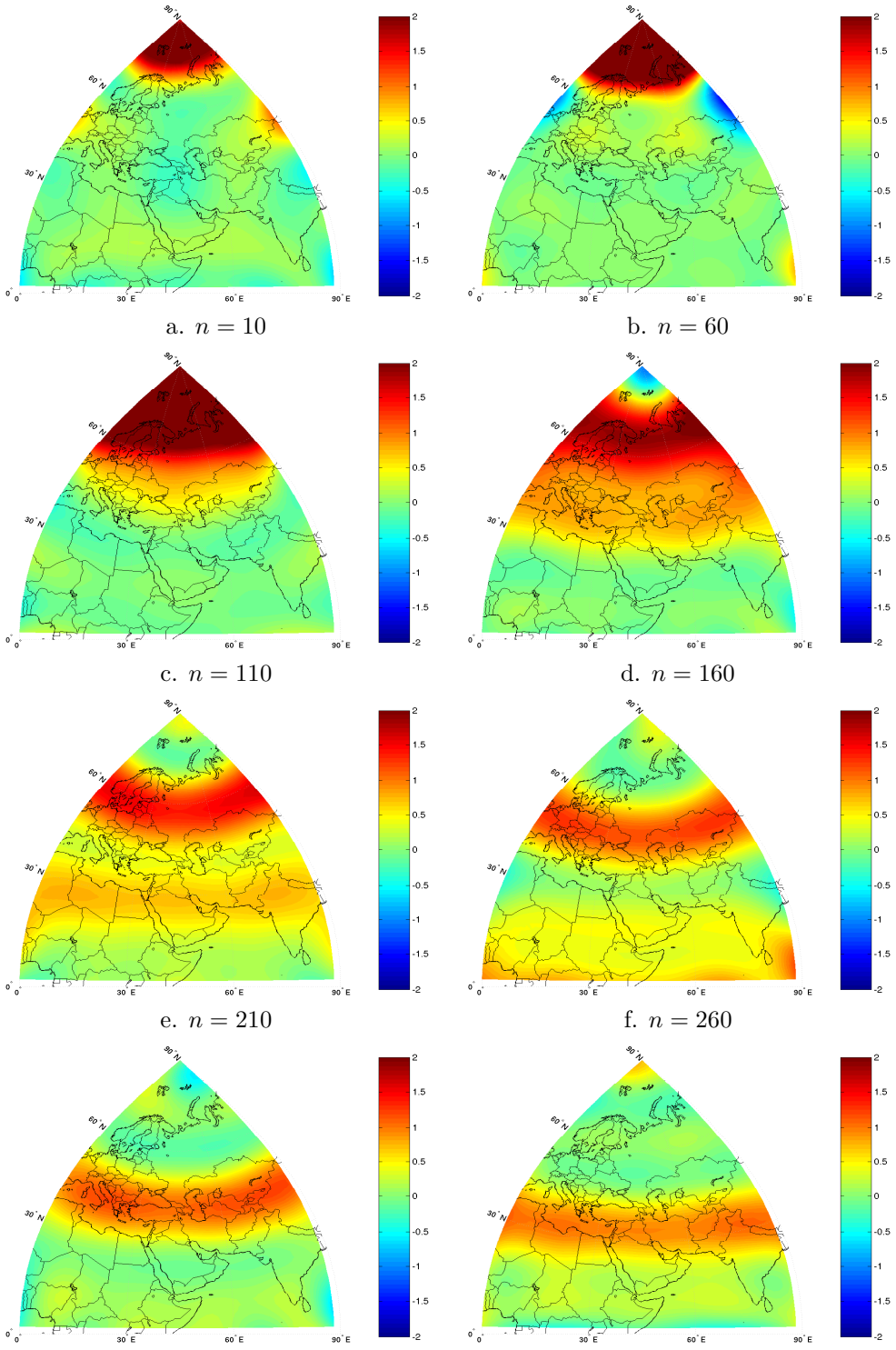

a. $n = 10$ b. $n = 60$

c. $n = 110$ d. $n = 160$

e. $n = 210$ f. $n = 260$

g. $n = 310$ h. $n = 360$

Figure 5: $S(t, x)$, truncated AP–kernel, $J = 2.8$, $\lambda = 10^{-2.5}$, $t = (-1 + (n-1)\,0.005)\,R/\alpha$.

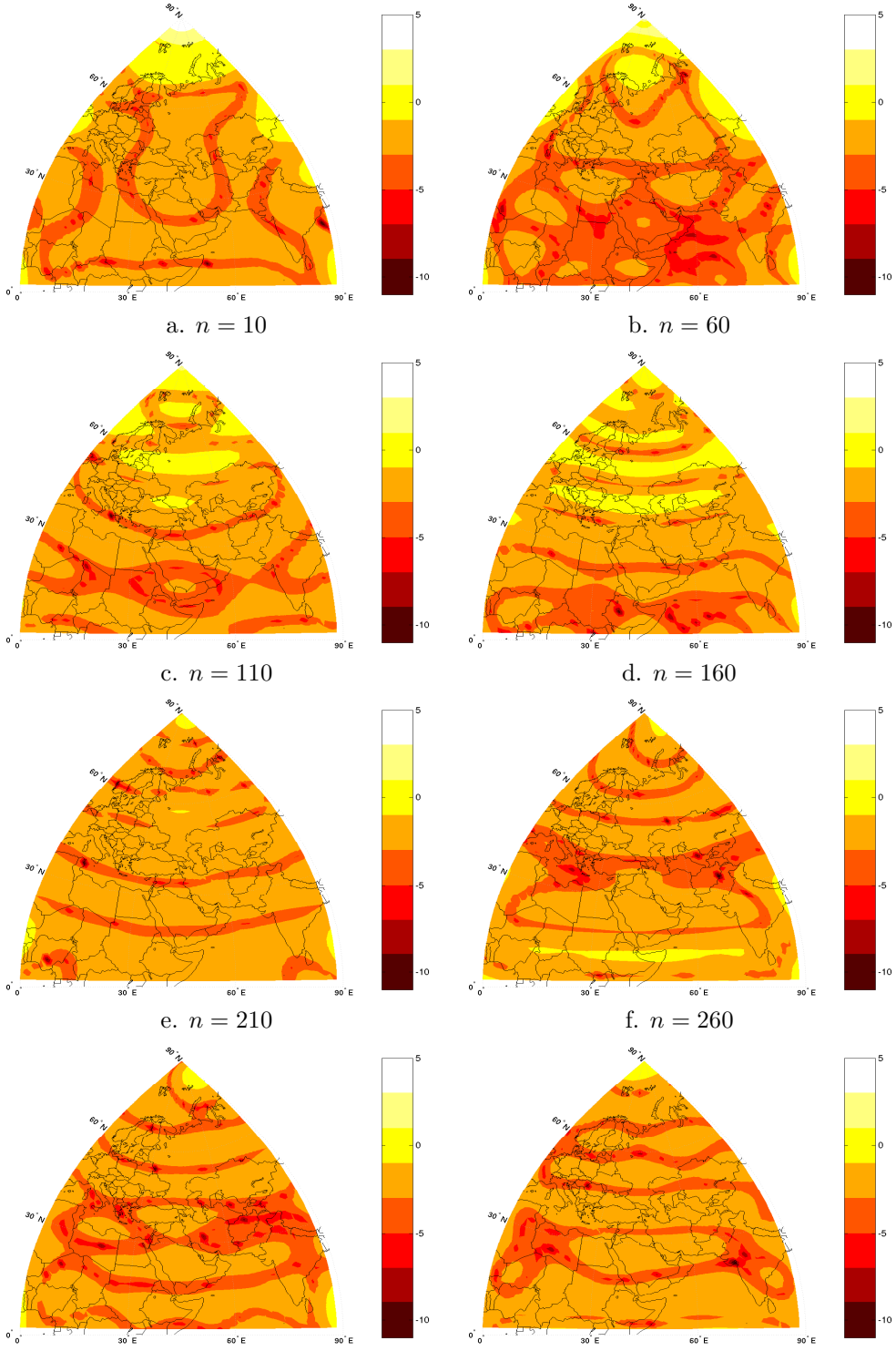

a. $n = 10$ b. $n = 60$

c. $n = 110$ d. $n = 160$

e. $n = 210$ f. $n = 260$

g. $n = 310$ h. $n = 360$

Figure 6: $\log(\,|S(t,x) - W(t,x)|\,)$, truncated AP–kernel, $J = 2.8$, $\lambda = 10^{-2.5}$, $t = (-1 + (n-1)\,0.005)\,R/\alpha$.

7.2 GEMINI

In the following section, we will use synthetic seismograms of an earthquake in Hokkaido, Japan (42.02° N, 142.55° E), which occurred on 26 November 1991. The seismograms were computed by the program system GEMINI written by Jörg Dalkolmo and Wolfgang Friederich (see [5]).

Following the procedure of the previous section, our first task is to construct an appropriate point grid in $\left]-\frac{R}{\alpha}, \frac{R}{\alpha}\right[\times \Omega_R$. We consider the time interval $[t_0, t_0 + 1400 \text{ s}]$, where $t_0 := -R/\alpha$ is the starting time of the earthquake and $t_0 + 1400 \text{ s} < R/\alpha$. GEMINI divides the time interval automatically into 180 equidistant samples. For our point grid every third point is chosen such that we obtain 60 separated points at intervals of about $23,5$ s.
We will now introduce another equidistributed point grid on the sphere, the so–called Brand grid (see [12]). Then we combine a Brand grid and a Reuter grid around the epicentre in order to receive a less evenly distributed point grid, which gives us a more realistic situation.

Definition 18 *A Brand grid on the unit sphere, dependent on the choice of a control parameter $\gamma \in \mathbb{N}$, is given by the points $(\varphi_{ij}, \vartheta_i)$ as follows:*

(i) $\vartheta_0 := 0$, $\varphi_{01} := 0$ *(North Pole),*

(ii) $\triangle\vartheta := \pi/\gamma$,

(iii) $\vartheta_i := i\triangle\vartheta$, $\quad 1 \le i \le \gamma - 1$,

(iv) $\gamma_i := 4i$, $\quad i \le \gamma/2$,
$\gamma_i := 4(\gamma - i)$, $\quad i > \gamma/2$,

(v) $\varphi_{ij} := (j-1)(2\pi/\gamma_i)$, $\quad 1 \le j \le \gamma_i$,

(vi) $\vartheta_\gamma := \pi$, $\varphi_{\gamma 1} := 0$ *(South Pole).*

Now we set $\gamma_{\text{Reuter}} = 25$ and $\gamma_{\text{Brand}} = 20$ and extract all points with $\vartheta \in]0, \pi/6[$. In this manner we obtain a Reuter grid of 59 points and a Brand grid of 24 points, both around the North Pole. Then the points are combined to one grid of 83 points and rotated in such a way that the centre of the grid is the epicentre $(\varphi, \vartheta) = (0.84, 2.5)$, which is equivalent to (42.02° N, 142.55° E). The resulting grid is shown in Figure 7.

For the following investigations we focus always on four certain gauging stations, which are located in increasing distance to the epicentre (see also Figure 8):

- station 1: $(\varphi, \vartheta) = (0.94, 2.59) \mathrel{\hat{=}} (35.9° \text{ N}, 148.4° \text{ E})$,
- station 2: $(\varphi, \vartheta) = (0.80, 2.16) \mathrel{\hat{=}} (43.9° \text{ N}, 123.7° \text{ E})$,
- station 3: $(\varphi, \vartheta) = (1.01, 2.92) \mathrel{\hat{=}} (31.7° \text{ N}, 167.2° \text{ E})$,
- station 4: $(\varphi, \vartheta) = (0.70, 1.84) \mathrel{\hat{=}} (49.7° \text{ N}, 105.7° \text{ E})$.

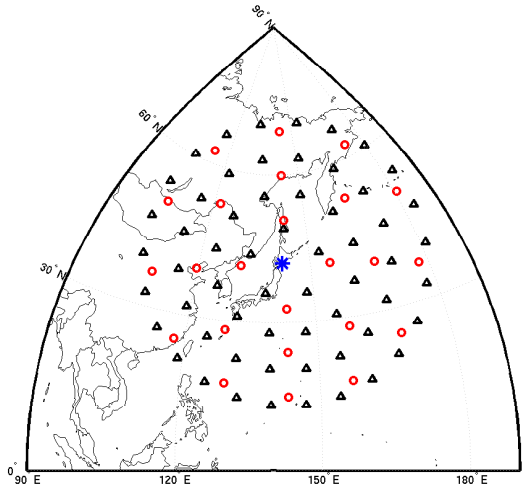

Figure 7: Reuter grid (triangles) and Brand grid (circles) around the epicentre (star).

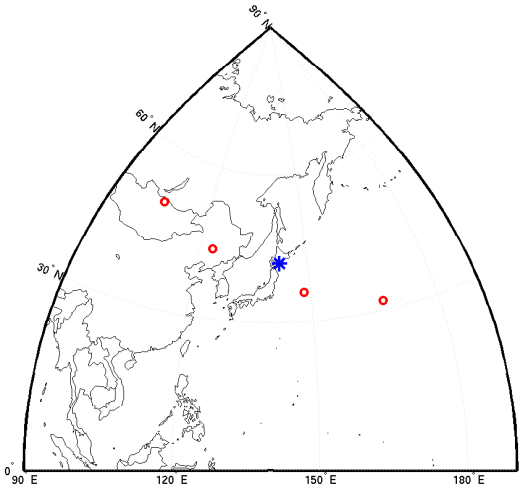

Figure 8: Epicentre (star) and stations 1–4 (circles).

At first we will fix $\lambda = 0.01$, i.e. we use little smoothing. Figure 9 shows the resulting spline obtained for $J = 7$. We observe that the wave is approximated rather well, but there are many oscillations in the whole time interval. This is due to the fact that a high J implies high polynomial degrees of the used basis functions, involving that one gets good interpolation, but also many oscillations.
Figure 10 describes the resulting spline for $J = 7$ and $\lambda = 1$. In comparison with Figure 9 we can see that the oscillations are much smaller now. In return, we have to accept that the wave amplitude is smaller, too, but it has not decreased as much as the oscillations.

Up to now we only involved the results at the gauging stations. If we plot the spline on the spatial domain we notice immediately that for $J = 7$ there are too many oscillations between the stations. Even with high smoothing there is no wave propagation recognisable. Therefore, we have to decrease the parameter J.
Further numerical tests yield that the best results in the spatial domain are obtained for $J = 4.5$. Moreover, we find out that $\lambda = 1$ is still too small and we have to set $\lambda = 2$ in order to get satisfactory results. Figure 11 shows the computed spline on the spatial domain for some fixed times. Here we can clearly see the propagation of the wave. Hence, we are able to determine the position of the wave front at an arbitrary time, although the spline does not give us the real amplitudes of the displacement. That was the primary intention of this work. Note that the typical structure of the wave front related to the NNE–SSW orientation of the tectonic fault is also visible. For further numerical results and comparison to other methods we refer to [15].

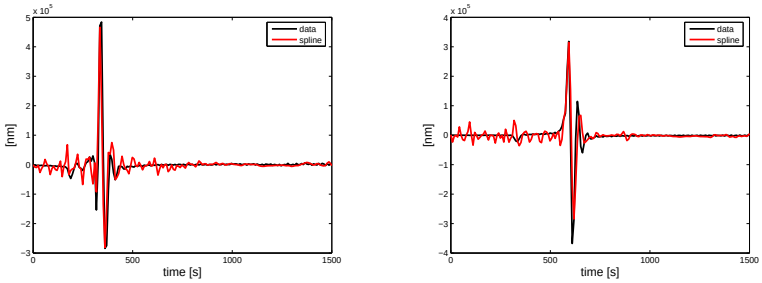

a. station 1 b. station 2

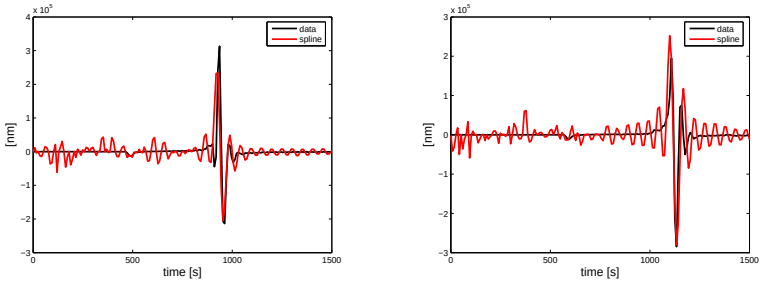

c. station 3 d. station 4

Figure 9: $S(t, x(R, \varphi, \vartheta))$, truncated AP–kernel, $J = 7$, $\lambda = 0.01$

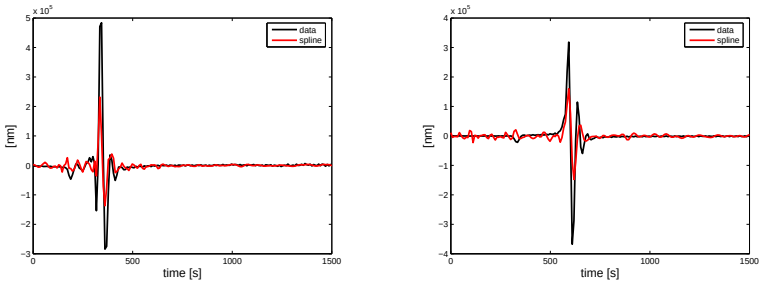

a. station 1 b. station 2

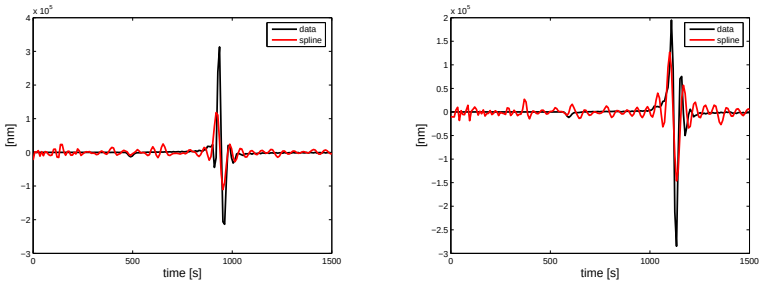

c. station 3 d. station 4

Figure 10: $S(t, x(R, \varphi, \vartheta))$, truncated AP–kernel, $J = 7$, $\lambda = 1$

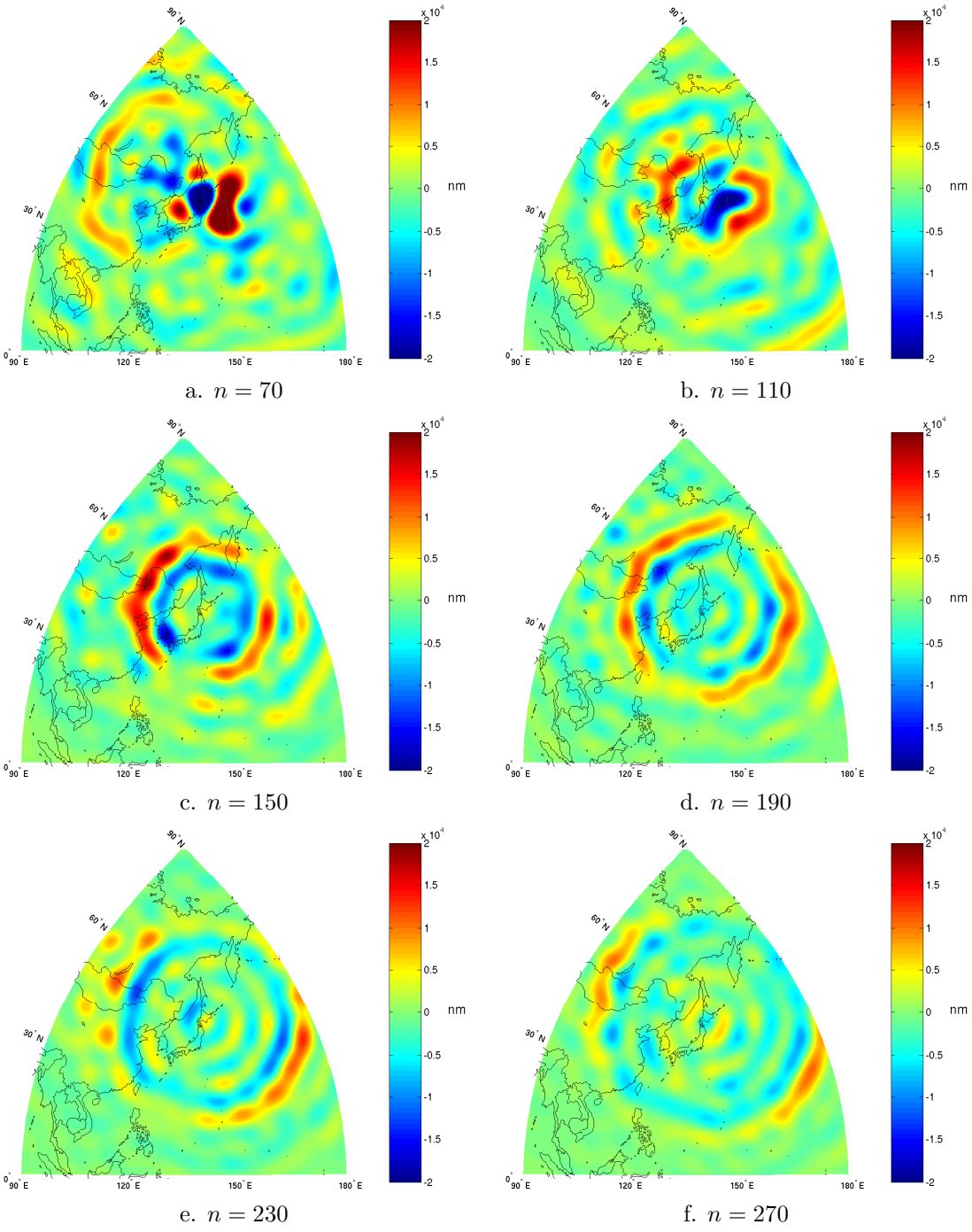

a. $n = 70$ b. $n = 110$

c. $n = 150$ d. $n = 190$

e. $n = 230$ f. $n = 270$

Figure 11: $S(t, x)$, $t = 4\,(n-1)$ s, truncated AP–kernel, $J = 4.5$, $\lambda = 2$.

8 Conclusions and Outlook

A spline method for the interpolation and approximation, respectively, of time– and space–dependent functions was introduced where the spatial part was assumed to be spherical in view of geoscientific, in particular seismic, applications. The background of this derivation is the Cauchy–Navier equation for isotropic, (layerwise) homogeneous media. Existence and uniqueness results as well as minimum properties and a convergence theorem were proved. Numerical tests with a known original wave function for a quantitative validation of the method and with realistic seismograms for a verification of the applicability to more intricate functions show good results including the ability of the approach to visualise the propagation of wave fronts.
The obtained results motivate further research in this field. The treatment of heterogeneous media as well as the inclusion of a priori information or boundary conditions, if known, in the modelling process are expected to be improvements.

References

[1] N. Aronszajn, *Theory of Reproducing Kernels*, Transactions of the American Mathematical Society **68** (1950), 337–404.

[2] A. Ben-Menahem and S.J.Singh, *Seismic Waves and Sources*, Springer, New York, Heidelberg, Berlin, 1981.

[3] V. Bolotnikov and L. Rodman, *Remarks on Interpolation in Reproducing Kernel Hilbert Spaces*, Houston Journal of Mathematics **30** (2004), 559–576.

[4] J. M. Brudowsky, *Über die elementare Darstellung von Cauchy-Navierschen Splines*, Diploma Thesis, Geomathematics Group, Department of Mathematics, University of Kaiserslautern, 1992.

[5] J. Dalkolmo, *Synthetische Seismogramme für eine sphärisch symmetrische, nichtrotierende Erde durch direkte Berechnung der Greenschen Funktion*, Diploma Thesis, Institut für Geophysik, Universität Stuttgart, 1993.

[6] P.J. Davis, *Interpolation and Approximation*, Dover Publications Inc., New York, 1975.

[7] M.J. Fengler, D. Michel, and V. Michel, *Harmonic Spline-Wavelets on the 3-dimensional Ball and their Application to the Reconstruction of the Earth's Density Distribution from Gravitational Data at Arbitrarily Shaped Satellite Orbits*, Zeitschrift für angewandte Mathematik und Mechanik (ZAMM), accepted for publication, 2006.

[8] W. Freeden, *On Approximation by Harmonic Splines*, Manuscripta Geodaetica **6** (1981), 193–244.

[9] W. Freeden, *On Spherical Spline Interpolation and Approximation*, Mathematical Methods in the Applied Sciences **3** (1981), 551–575.

[10] W. Freeden, *Metaharmonic Splines for Solving the Exterior Dirichlet Problem for the Helmholtz Equation*, Topics in Multivariate Approximation (C.K. Chui F. Utreras and L.L. Schumaker, eds.), Academic Press, 1987, pp. 99–110.

[11] W. Freeden, *Multiscale Modelling of Spaceborne Geodata*, Teubner, Stuttgart, Leipzig, 1999.

[12] W. Freeden, T. Gervens, and M. Schreiner, *Constructive Approximation on the Sphere (With Applications to Geomathematics)*, Oxford Science Publications, Clarendon, 1998.

[13] W. Freeden and V. Michel, *Multiscale Potential Theory (with Application to Geoscience)*, Birkhäuser, Boston, 2004.

[14] W. Freeden, M. Schreiner, and R. Franke, *A Survey on Spherical Spline Approximation*, Surveys on Mathematics for Industry **7** (1997), 29–85.

[15] P. Kammann, *Modelling Seismic Wave Propagation Using Time-Dependent Cauchy-Navier Splines*, Diploma Thesis, Geomathematics Group, Department of Mathematics, University of Kaiserslautern, 2005.

[16] V. Michel, *Theoretical Aspects of a Multiscale Analysis of the Eigenoscillations of the Earth*, Revista Matemática Complutense **16** (2003), 519–554.

[17] C. Müller, *Über die ganzen Lösungen der Wellengleichung*, Mathematische Annalen **124** (1952), 235–264.

[18] R. Reuter, *Über Integralformeln der Einheitssphäre und harmonische Splinefunktionen*, Veröffentlichungen des Geodätischen Instituts, RWTH Aachen, Heft 33, 1982.

[19] S. Saitoh, *Best Approximation, Tikhonov Regularization and Reproducing Kernels*, Kodai Mathematical Journal **28** (2005), 519–554.

[20] S. Saitoh, T. Matsuura, and M. Asaduzzaman, *Operator Equations and Best Approximation Problems in Reproducing Kernel Hilbert Spaces*, Journal of Analysis and Applications **1** (2003), 131–142.

[21] H.R. Schwarz, *Numerische Mathematik*, B.G.Teubner, Stuttgart, 1997.

[22] M. Tücks, *Navier-Splines und ihre Anwendung in der Deformationsanalyse*, PhD Thesis, Geomathematics Group, Department of Mathematics, University of Kaiserslautern, Shaker, Aachen, 1996.

[23] W. Walter, *Einführung in die Theorie der Distributionen*, 3rd ed., BI-Wissenschafts-Verlag, Mannheim, 1994.

[24] K. Wolf, *Numerical Aspects of Harmonic Spline-Wavelets for the Satellite Gravimetry Problem*, Diploma Thesis, Geomathematics Group, Department of Mathematics, University of Kaiserslautern, 2006.

Folgende Berichte sind erschienen:

2003

Nr. 1 S. Pereverzev, E. Schock.
On the adaptive selection of the parameter in regularization of ill-posed problems

Nr. 2 W. Freeden, M. Schreiner.
Multiresolution Analysis by Spherical Up Functions

Nr. 3 F. Bauer, W. Freeden, M. Schreiner.
A Tree Algorithm for Isotropic Finite Elements on the Sphere

Nr. 4 W. Freeden, V. Michel (eds.)
Multiscale Modeling of CHAMP-Data

Nr. 5 C. Mayer
Wavelet Modelling of the Spherical Inverse Source Problem with Application to Geomagnetism

2004

Nr. 6 M.J. Fengler, W. Freeden, M. Gutting
Darstellung des Gravitationsfeldes und seiner Funktionale mit Multiskalentechniken

Nr. 7 T. Maier
Wavelet-Mie-Representations for Soleniodal Vector Fields with Applications to Ionospheric Geomagnetic Data

Nr. 8 V. Michel
Regularized Multiresolution Recovery of the Mass Density Distribution From Satellite Data of the Earth's Gravitational Field

Nr. 9 W. Freeden, V. Michel
Wavelet Deformation Analysis for Spherical Bodies

Nr. 10 M. Gutting, D. Michel (eds.)
Contributions of the Geomathematics Group, TU Kaiserlautern, to the 2nd International GOCE User Workshop at ESA-ESRIN Frascati, Italy

Nr. 11 M.J. Fengler, W. Freeden
A Nonlinear Galerkin Scheme Involving Vector and Tensor Spherical Harmonics for Solving the Incompressible Navier-Stokes Equation on the Sphere

Nr. 12 W. Freeden, M. Schreiner
Spaceborne Gravitational Field Determination by Means of Locally Supported Wavelets

Nr. 13 F. Bauer, S. Pereverzev
Regularization without Preliminary Knowledge of Smoothness and Error Behavior

Nr. 14 W. Freeden, C. Mayer
Multiscale Solution for the Molodensky Problem on Regular Telluroidal Surfaces

Nr. 15 W. Freeden, K. Hesse
Spline modelling of geostrophic flow: theoretical and algorithmic aspects

2005

Nr. 16 M.J. Fengler, D. Michel, V. Michel
Harmonic Spline-Wavelets on the 3-dimensional Ball and their Application to the Reconstruction of the Earth's Density Distribution from Gravitational Data at Arbitrarily Shape Satellite Orbits

Nr. 17 F. Bauer
Split Operators for Oblique Boundary Value Problems

Nr. 18 W. Freeden, M. Schreiner
Local Multiscale Modelling of Geoidal Undulations from Deflections of the Vertical

Nr. 19 W. Freeden, D. Michel, V. Michel
Local Multiscale Approximations of Geostrophic Flow: Theoretical Background and Aspects of Scientific Computing

Nr. 20 M.J. Fengler, W. Freeden, M. Gutting
The Spherical Bernstein Wavelet

Nr. 21 M.J. Fengler, W. Freeden,
A. Kohlhaas, V. Michel, T. Peters
Wavelet Modelling of Regional and Temporal Variations of the Earth's Gravitational Potential Observed by GRACE

Nr. 22 W. Freeden, C. Mayer
A Wavelet Approach to Time-Harmonic Maxwell's Equations

Nr. 23 M.J. Fengler, D. Michel, V. Michel
Contributions of the Geomathematics Group to the GAMM 76th Annual Meeting

Nr. 24 F. Bauer
Easy Differentiation and Integration of Homogeneous Harmonic Polynomials

Nr. 25 T. Raskop, M. Grothaus
On the Oblique Boundary Problem with a Stochastic Inhomogeneity

2006

Nr. 26 P. Kammann, V. Michel
Time-Dependent Cauchy-Navier Splines and their Application to Seismic Wave Front Propagation

TECHNISCHE UNIVERSITÄT
KAISERSLAUTERN

Informationen:

Prof. Dr. W. Freeden
Prof. Dr. E. Schock
Fachbereich Mathematik
Technische Universität Kaiserslautern
Postfach 3049
D-67653 Kaiserslautern
E-Mail: freeden@mathematik.uni-kl.de
schock@mathematik.uni-kl.de